SANDIA NATIONAL LABORATORIES
WASTE ISOLATION PILOT PLANT

DIRECT BRINE RELEASE ANALYSIS REPORT FOR THE REPLACEMENT PANELS PLANNED CHANGE REQUEST (RPPCR)

REVISION 0

Author:	Paul Docherty	*Signature on File*	11/7/2023
	Print	Signature	Date
Author:	Seth King		11/7/2023
	Print	Signature	Date
Technical Reviewer:	James Bethune	*Signature on File*	11/7/2023
	Print	Signature	Date
QA Reviewer:	Shelly Nielsen	Shelly R. Nielsen	11-7-2023
	Print	Signature	Date
Management Reviewer:	Steve Wagner		11/7/2023
	Print	Signature	Date

ERMS #579724

NOVEMBER 2023

WIPP:4.4.1.2.1:PA:QA-L:578831

Information Only

This page intentionally left blank.

Information Only

Executive Summary

As currently permitted, the Waste Isolation Pilot Plant (WIPP) includes ten excavated panels for the placement of waste. For operational reasons, not all of the volume of the ten excavated panels will be used for waste disposal. The DOE plans to submit a Planned Change Request (PCR) to excavate two panels, termed replacement panels, to provide an equivalent disposal capability, and may consider excavating up to seven panels beyond the two replacement panels, defined here as additional panels. The Replacement Panels Planned Change Request Performance Assessment (RPPCR PA) has been executed by Sandia National Laboratories (SNL) to quantify the long-term performance of the repository with both replacement and additional panels. Results from the RPPCR are compared to those obtained in the 2019 Compliance Recertification Application (CRA-2019) (Zeitler et al. 2019) in order to assess repository performance in terms of the most recent regulatory submittal.

This analysis report documents the Direct Brine Release (DBR) component of the RPPCR. Changes incorporated into the RPPCR include inventory updates, changes related to the replacement and additional panels, an update to the porosity surface used to represent creep closure in the Salado, routine updates due to new information and model revisions since the CRA-2019 PA, and updates to the PA codes and computing platform.

For the RPPCR, the number of simulations with non-zero DBR increased; however, there were significantly more simulations with small magnitude releases compared to the CRA-2019. The number of simulations with large magnitude releases decreased in the RPPCR. In addition, the mean DBR volume fell by a factor of three in the RPPCR compared to the CRA-2019.

Down-dip intrusion locations in the south contributed the bulk of DBR volumes, as was the case in the CRA-2019. The RPPCR included a new intrusion location not present in the CRA-2019. The new intrusion, being the farthest up-dip and farthest away from any previous intrusions, produced the lowest releases of all the intrusion locations.

A major driver for changes in DBR volumes from the CRA-2019 to the RPPCR is the updated porosity surface used in BRAGFLO to determine pressure and brine saturation in the waste, which are initial conditions for DBR simulations. The new porosity surface significantly reduces porosity in the waste compared to the CRA-2019, affecting both initial waste pressure and brine saturation in the RPPCR DBR simulations.

Information Only

TABLE OF CONTENTS

EXECUTIVE SUMMARY ..... **III**

1.0 INTRODUCTION **1**

1.1 Changes Since the CRA-2019 2

2.0 CONCEPTUAL APPROACH FOR THE RPPCR **5**

2.1 Model Geometry 7

2.2 Initial Conditions 9

3.0 DBR METHODOLOGY **11**

3.1 Modeled Scenarios 11

3.2 Code Execution and Run Control 11

4.0 RESULTS **13**

4.1 Summary 13

4.2 S1-DBR 18

4.3 S2-DBR 21

4.4 S4-DBR 23

4.5 Maximum Releases 26

5.0 DRIVERS AND CORRELATIONS **27**

5.1 Initial Conditions Summary 27

5.2 Correlation and Sensitivity to Initial Conditions 31

5.3 Comparison to Other Analyses 36

6.0 SUMMARY **39**

7.0 REFERENCES **41**

8.0 APPENDIX A: SENSITIVITY TO INPUT PARAMETERS **43**

LIST OF TABLES

Table 1 – Summary of PA parameters used to compute DBR volumes 6

Table 2 – DBR Scenarios 11

Table 3 – DBR volume summary 15

Information Only

Table 4 – S1-DBR volume summary 19
Table 5 – S2-DBR volume summary 22
Table 6 – S4-DBR volume summary 24
Table 7 – Largest DBR volumes by analysis 26
Table 8 – S2-DBR mean initial conditions. 28
Table 9 – DBR volume summary 36

LIST OF FIGURES

Figure 1: CRA-2019 DBR grid with simulated intrusion locations. 8
Figure 2: RPPCR DBR grid with simulated intrusion locations 9
Figure 3: Regions used to transfer initial pressure and saturation from the BRAGFLO Salado grid to the DBR grid. 10
Figure 4: DBR run control diagram. 12
Figure 5: Release volume frequency, all non-zero releases 16
Figure 6: Release volume frequency, L, M, and U non-zero releases only 16
Figure 7: Release volumes, all non-zero releases 17
Figure 8: Release volumes by scenario, all non-zero releases 17
Figure 9: Number of non-zero DBR events by scenario 18
Figure 10: S1-DBR release volumes, all non-zero releases 20
Figure 11: S2-DBR release volumes, all non-zero releases 23
Figure 12: S4-DBR releases volumes, all non-zero releases 25
Figure 13: S2-DBR brine pressure, all intrusions. 29
Figure 14: S2-DBR brine saturation, all intrusions 30
Figure 15: S2-DBR release volume versus brine pressure, all non-zero intrusions 33
Figure 16: S2-DBR release volume versus brine saturation, all non-zero intrusions 34
Figure 17: Brine saturation frequency, S2-DBR all Lower and Middle intrusions 35
Figure 18: Brine saturation frequency, S2-DBR all Upper and Other intrusions 35
Figure 19: Brine release volumes for all non-zero DBRs. 37
Figure 20: Halite porosity versus brine release volume for Location "L", Scenario S2-DBR, time 10,000 years 44
Figure 21: Borehole permeability versus brine release volume for Location "L", Scenario S2-DBR, time 10,000 years 44
Figure 22: DRZ permeability versus brine release volume for Location "L", Scenario S2-DBR, time 10,000 years 45

Information Only

Figure 23: Castile brine pressure versus brine release volume for Location "L", Scenario S2-DBR, time 550 years.....45

Information Only

1.0 INTRODUCTION

The Waste Isolation Pilot Plant (WIPP), located in southeastern New Mexico, has been developed by the U.S. Department of Energy (DOE) for the geologic (deep underground) disposal of transuranic (TRU) waste. Containment of TRU waste at the WIPP is regulated by the U.S. Environmental Protection Agency (EPA) according to the regulations set forth in Title 40 of the Code of Federal Regulations (CFR), Part 191.

The DOE demonstrates compliance with the containment requirements according to the Certification Criteria in Title 40 CFR Part 194 by means of performance assessment (PA) calculations performed by Sandia National Laboratories (SNL). WIPP PA calculations estimate the probability and consequence of potential radionuclide releases from the repository to the accessible environment for a regulatory period of 10,000 years after facility closure. The models used in PA are maintained and updated with new information as part of an ongoing process. Improved information regarding important WIPP features, events, and processes typically results in refinements and modifications to PA models and the parameters used in them. Planned changes to the repository and/or the components therein also result in updates to WIPP PA models. WIPP PA models are used to support the repository recertification process that occurs at five-year intervals following the receipt of the first waste shipment at the site in 1999.

PA calculations were included in the 1996 Compliance Certification Application (CCA) (U.S. DOE 1996), and in a subsequent Performance Assessment Verification Test (PAVT) (MacKinnon and Freeze 1997a, 1997b and 1997c). Based in part on the CCA and PAVT PA calculations, the EPA certified that the WIPP met the regulatory containment criteria. The facility was approved for disposal of transuranic waste in May 1998 (U.S. EPA 1998). Subsequent CRA PA submittals including the CRA-2004, CRA-2009, CRA-2014, and CRA-2019 have included PA calculations. EPA requested additional PA calculations, termed Performance Assessment Baseline Calculations (PABC) for the CRA-2004 and CRA-2009 submittals before recertification. The EPA conducted a separate analysis, termed CRA19-COMB, based on the CRA-2019 PA with several different assumptions and models (Section 4.6, EPA 2022a).

As currently permitted, the WIPP includes ten excavated panels for the placement of waste. For operational reasons, not all of the volume of the ten excavated panels will be used for waste disposal. The DOE plans to submit a Planned Change Request (PCR) to excavate two panels, termed replacement panels, to provide an equivalent disposal capability, and may consider excavating up to seven panels beyond the two replacement panels, defined here as additional panels. SNL executed the Replacement Panels Planned Change Request (RPPCR) PA to quantify the long-term performance of the repository with the replacement and additional panels in support of the DOE's submittal of the PCR. The PA executed in support of the RPPCR is detailed in AP-204 (Hansen et al. 2023). Results found in the RPPCR are compared to those obtained in the 2019 Compliance Recertification Application (CRA-2019) (Zeitler et al. 2019).

Changes incorporated into this analysis include inventory updates, changes related to the replacement and additional panels, routine updates due to new information and model revisions since the CRA-2019 PA, and updates to the PA codes and computing platform. This analysis report documents the Direct Brine Release (DBR) component of the RPPCR PA.

Information Only

1.1 Changes Since the CRA-2019

A number of changes are incorporated in the RPPCR relative to the CRA-2019 PA that potentially impact DBR results. The changes are:

- Updates to repository area and volume parameters to account for new panels.
- Changes to DBR grid representation to account for new waste areas.

There are also several changes incorporated into the RPPCR relative to the CRA-2019 PA that potentially impact the DBR results by impacting conditions from the Salado flow calculation. These changes are:

- Modified grid for the Salado flow model.
- Updated porosity surface used to represent creep closure of excavations in the Salado.
- Changes to pressure at repository at closure.
- New methodology for calculating iron surface area used for gas generation from iron corrosion.
- Updated permeability of a borehole after plug failure and degradation of borehole materials to take into account a re-analysis of wellbore materials.
- Updates to waste inventory parameters.
- Updates to actinide baseline solubilities and solubility uncertainty distributions.
- Revised model for the oxidation states of actinides.
- Updated model inputs describing the Castile brine reservoir to account for a recent re-analysis of Castile reservoir data.

In addition, there are changes related to codes and the computing platform:

- Hardware and computational code updates.

Two key changes listed above that affect DBRs in the RPPCR analysis are (i) changes to the DBR numerical grid to account for new waste areas; and (ii) updates to the porosity surface used to represent creep closure of excavations in the Salado. The DBR numerical grid for the RPPCR takes a conceptual deviation from the CRA-2019 DBR grid. In the CRA-2019 DBR grid, and previous DBR grids, the entire waste volume was modeled. For the RPPCR, the intruded waste panel volume and any volume not separated by a panel closure to the intruded waste panel are modeled, however not all of the volume of the waste area is modeled. Analyses have shown that direct brine release volumes are primarily determined by the conditions in the intruded panel; other areas in the DBR grid have little to no effect on DBRs (Shumaker, 2021). This is due to the DBR simulation time being of short duration, which results in very little communication across panel closures. With this assumption, the North Rest-of-Repository in the CRA-2019 DBR grid has been split into two regions, and intrusions into the two regions are modeled separately. The major assumptions associated with these changes to the DBR grid were implemented in the Additional Panels Performance Assessment, or APPA (King, 2021; Brunell et al., 2021), and were reviewed by the APPA Changed Conceptual Models Peer Review. The peer review panel found the assumptions to be well justified and the model adequate and reasonable for its intended application (Falta et al., 2021). With the conclusions from the peer review panel, these conceptual models are used in the RPPCR.

Information Only

The second key change affecting DBRs in the RPPCR, the updated porosity surface, causes porosity in the waste areas to fall significantly so that final pore volume in the waste is only half that seen in the CRA-2019 (King, 2023). This decrease in realized porosities is a major driver for changes in pressure and brine saturation seen in the Salado flow simulations. Pressure and saturation from the Salado flow simulations are initial conditions in the DBR calculation: changes to these initial conditions in the RPPCR strongly affect both the number of DBRs and the volume of brine released in a DBR.

Information Only

This page intentionally left blank.

Information Only

2.0 CONCEPTUAL APPROACH FOR THE RPPCR

If the WIPP repository were to be penetrated by a borehole while under conditions of sufficient repository brine pressure and saturation, brine could migrate up through the intruding borehole to reach the land surface. Such an event is defined as a DBR. As with previous WIPP PAs, the BRAGFLO DBR analysis uses the BRAGFLO code to numerically evaluate the volumetric flux of brine that enters the borehole over the duration of the release using the well deliverability equations (Mattax and Dalton, 1990):

$$\text{DBR volume} = \int_0^{t_e} q_b(t)\,dt = \int_0^{t_e} J_b\left[p_b(t) - p_{wf}\right] dt \quad . \tag{1}$$

In equation (1):

- t elapsed time since drilling intrusion [s];
- t_e duration of the DBR event [s];
- $q_b(t)$ volumetric flux [m^3/s] of brine into the intrusion as a function of time;
- J_b well productivity index [m^3/(Pa·s)];
- $p_b(t)$ brine pressure [Pa] calculated by BRAGFLO at the location of the intrusion; and
- p_{wf} flowing bottom-hole pressure [Pa].

The duration of the DBR event (t_e) is between 3 and 4.5 days. After 3 days, if at any time the gas flowrate in the borehole falls below the gas cut-off rate of 100 mscf/day (2832 m^3/day) it is assumed the well would be cased and the DBR event ends at that time. If the gas flow rate remains above the cut-off rate, it is assumed the well could be brought under control after 4.5 days, ending the DBR event (Kirkes, 2007).

Values for the flowing bottom-hole pressure, p_{wf}, were previously tabulated through an iterative calculation assuming equilibrium with atmospheric pressure at the ground surface for a range of repository pressures and saturations. Curve fit functions of these tables were then created for different flow regimes (all-brine, brine-dominated, and gas-dominated). The flowing bottom-hole pressure is calculated from these look-up table fit functions (Stoelzel and O'Brien, 1996).

The well productivity index, J_b, is a measure of how readily brine can enter the well. In a radial drainage area with uniform saturation, it can be determined from Darcy's law (Chappelear and Williamson, 1981):

$$J_b = \frac{2\pi k k_r h}{\mu[ln(r_e/r_w)+s-0.5]} \quad . \tag{2}$$

In equation (2):

- k intrinsic permeability of the waste [m^2];
- k_r relative permeability of the waste to brine [--];
- h height of the crushed panel [m];
- μ brine viscosity [Pa·s];
- r_e effective drainage radius of the intruded cell [m];
- r_w radius of the wellbore [m]; and

Information Only

s skin factor [--].

Relative permeability is computed using the model of Brooks and Corey (1964) given by $k_r = S_e^{3+2/\lambda}$ where λ is the pore distribution parameter, $S_e = (S_b - S_{br})/(1 - S_{br})$ is the effective brine saturation, S_b is the brine saturation at the time of the intrusion, and S_{br} is the residual brine saturation. The crushed panel height is defined as $h = h_i(1 - \phi_i)/(1 - \phi)$, where h_i and ϕ_i are the initial height and porosity of the waste and ϕ is the volume-averaged porosity of the waste at the time of intrusion (Helton et al., 1998). The effective drainage radius is defined by $r_e = \sqrt{\Delta x \Delta y/\pi}$, where Δx and Δy are the dimensions of the grid cell containing the well (see Figure 2). The wellbore radius is fixed at 0.1556 m, based on the assumption of a 12.25 in. drill bit diameter. Lastly, as described by Helton et al. 1998, skin factor s is used to incorporate flow stimulation caused by spallings release: $s = -ln\left[\sqrt{\frac{V_i}{\pi h_i}}/r_w\right]$, where V_i is the uncompacted volume of spallings material. Note that J_b is constant for a particular drilling intrusion and that in Equation 1 only brine pressure $p_b(t)$ is a function of time.

The PA parameter values used to compute the DBR volumes are summarized in Table 1. All except the residual brine saturation in the waste are constant.

Table 1 – Summary of PA parameters used to compute DBR volumes

PA Parameter	Description	Value
WAS_AREA:PRMX_LOG	Intrinsic permeability of the waste (k)	2.4×10^{-13} m^2
WAS_AREA:PORE_DIS	Brooks-Corey pore distribution parameter (λ)	2.89
WAS_AREA:SAT_RBRN	Residual brine saturation in the waste (S_{br})	Uniform distribution Max: 0.552 Mean 0.276 Min 0.000
WAS_AREA:POROSITY	Initial waste porosity (ϕ_i)	0.848
BRINESAL:VISCO	Brine dynamic viscosity (μ)	0.0021 Pa·s
BOREHOLE:DIAMMOD	Drill bit diameter ($2 \times r_w$)	0.311 m
BLOWOUT:HREPO	Initial waste panel height (h_i)	3.96 m
BLOWOUT:MINFLOW	Minimum duration of DBR	3 days
BLOWOUT:MAXFLOW	Maximum duration of DBR	4.5 days
BLOWOUT:GAS_MIN	Gas cut-off rate	2832 m^3/day

As defined for WIPP PA, minimum pressure and saturation conditions must exist within the waste panel for brine to flow to the surface during an intrusion and produce a DBR. Pressure in the intruded waste panel must be great enough to overcome the static pressure exerted by a column of drilling fluid at the repository depth, assumed to be equal to 8 megapascals (MPa). Brine saturation in the intruded waste panel must be above the residual brine saturation of the waste, that is, the brine must be mobile.

Information Only

2.1 Model Geometry

The BRAGFLO_DBR model explicitly represents the vicinity of the waste panels, including specific repository features like individual panels and panel closures, in a 2-dimensional rectilinear grid. Like the BRAGFLO Salado Model (King, 2023), the grid dips 1° to the south.

The DBR numerical grid and material map used in the CRA-2019 PA calculations are shown in Figure 1 and the DBR numerical grid and material map used in the RPPCR calculations are shown in Figure 2. As mentioned in Section 1.1, the North Rest-of-Repository in the CRA-2019 DBR grid has been split into two regions for the RPPCR.

In addition to the three drilling locations considered in the CRA-2019 PA, a fourth intrusion location is considered in the RPPCR. An "O" (for other) intrusion location has been added to the existing locations "U" (for upper, since it is up-dip), "M" (for middle), and "L" (for lower, since it is down-dip). These intrusion locations are shown in Figure 2. Some of the DBR calculations are for a drilling intrusion preceded by an E1 intrusion in either the same or a different waste panel. An E1 intrusion is a borehole that intersects the repository and then continues down to penetrate a hypothetical brine reservoir. The effects of a prior E1 intrusion are incorporated into the calculations by specifying pressure at a boundary condition well. The location of the boundary condition well is denoted by the red dot in Figure 1 and Figure 2. Properties of the boundary condition well depend on the amount of time that has elapsed since the previous E1 intrusion occurred, as this determines whether the borehole between the repository and the brine reservoir is open, contains fill, or is closed due to salt creep. Helton et al. 1998 give formulas for determining the boundary well pressure under the different borehole conditions.

Information Only

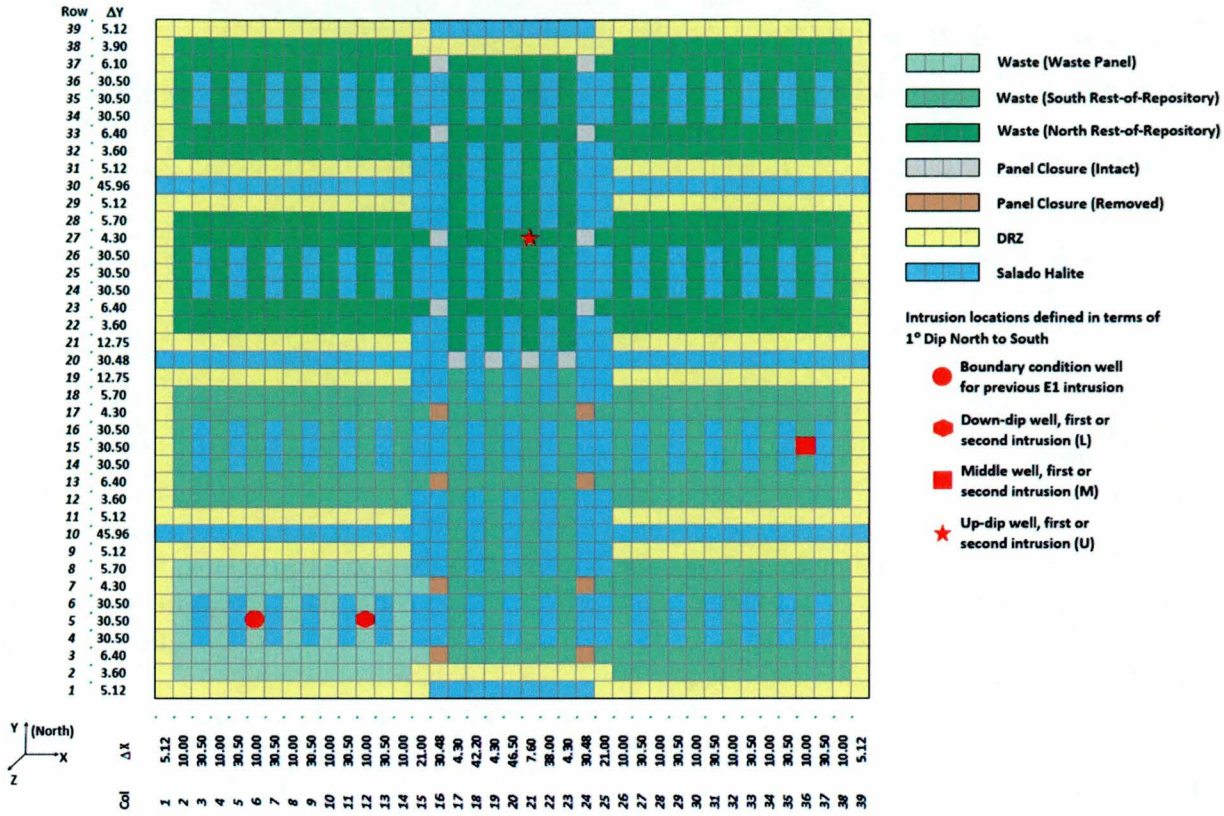


Figure 1: CRA-2019 DBR grid with simulated intrusion locations.

Information Only

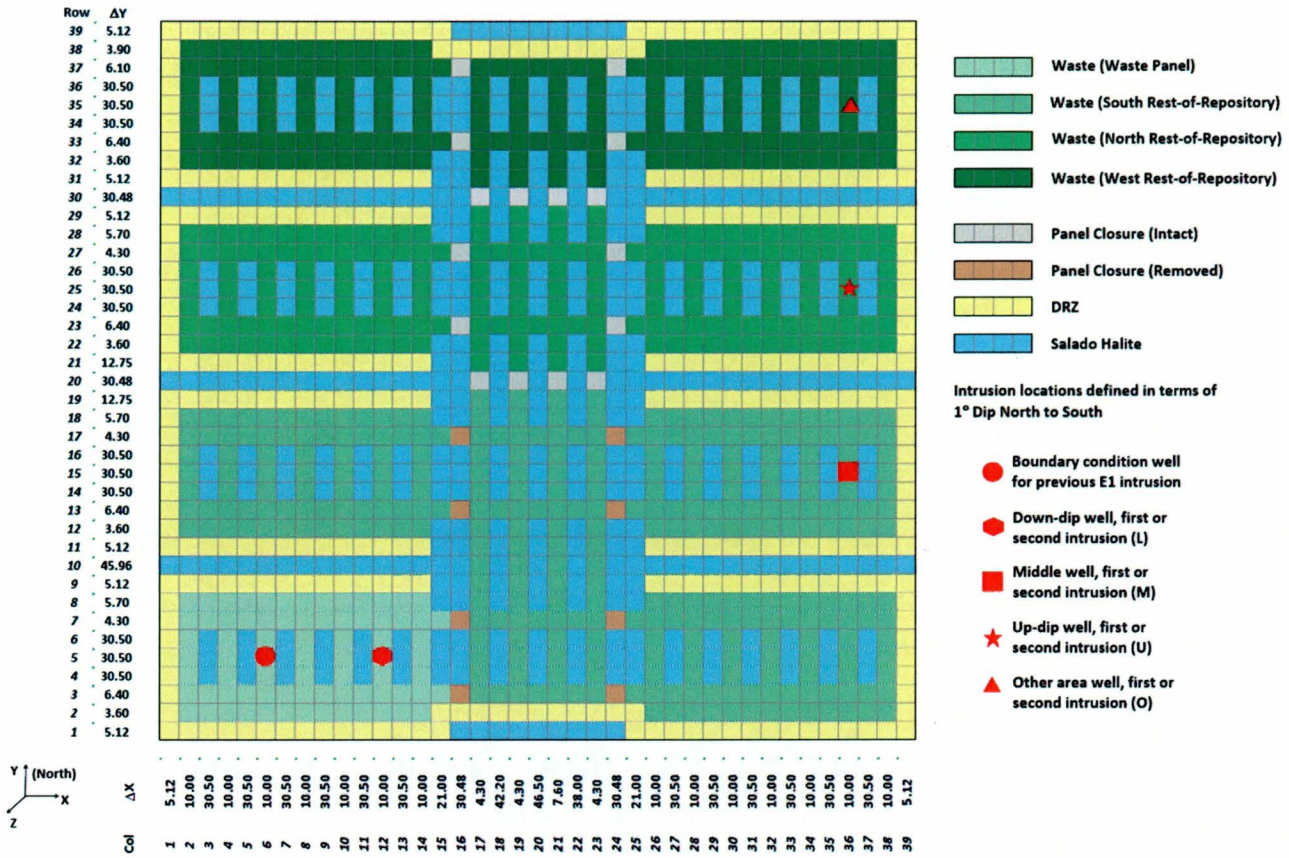


Figure 2: RPPCR DBR grid with simulated intrusion locations.

2.2 Initial Conditions

Brine pressures and brine saturations calculated during the BRAGFLO Salado flow simulations (King, 2023) are volume-averaged and used as initial conditions in the DBR simulations. Figure 3 illustrates the method used to transfer initial conditions in the waste for the RPPCR. The BRAGFLO grid aggregates waste panels into four waste-bearing regions: Waste Panel, South Rest of Repository, North Rest of Repository, and West Rest of Repository (Hansen, 2023). In Figure 3, these regions are denoted Waste Panel, SRoR, NRoR and WRoR, respectively. At the time of the intrusion, the volume-averaged pressure and saturation from the four waste-filled regions in the BRAGFLO grid are used as the initial pressure and saturation for corresponding waste regions in the DBR grid. Consistent with the designations L, M, U and O for the intrusion locations, the DBR grid waste regions will be referred to as Lower, Middle, Upper, and Other. As indicated in Figure 3, conditions in the BRAGFLO Waste Panel map to the Lower waste region in the DBR grid; likewise, BRAGFLO SRoR conditions map to the Middle DBR region, NRoR to the Upper DBR region, and WRoR to the Other DBR region. Note that pressure and saturation are allowed to change during the DBR calculations.

Information Only

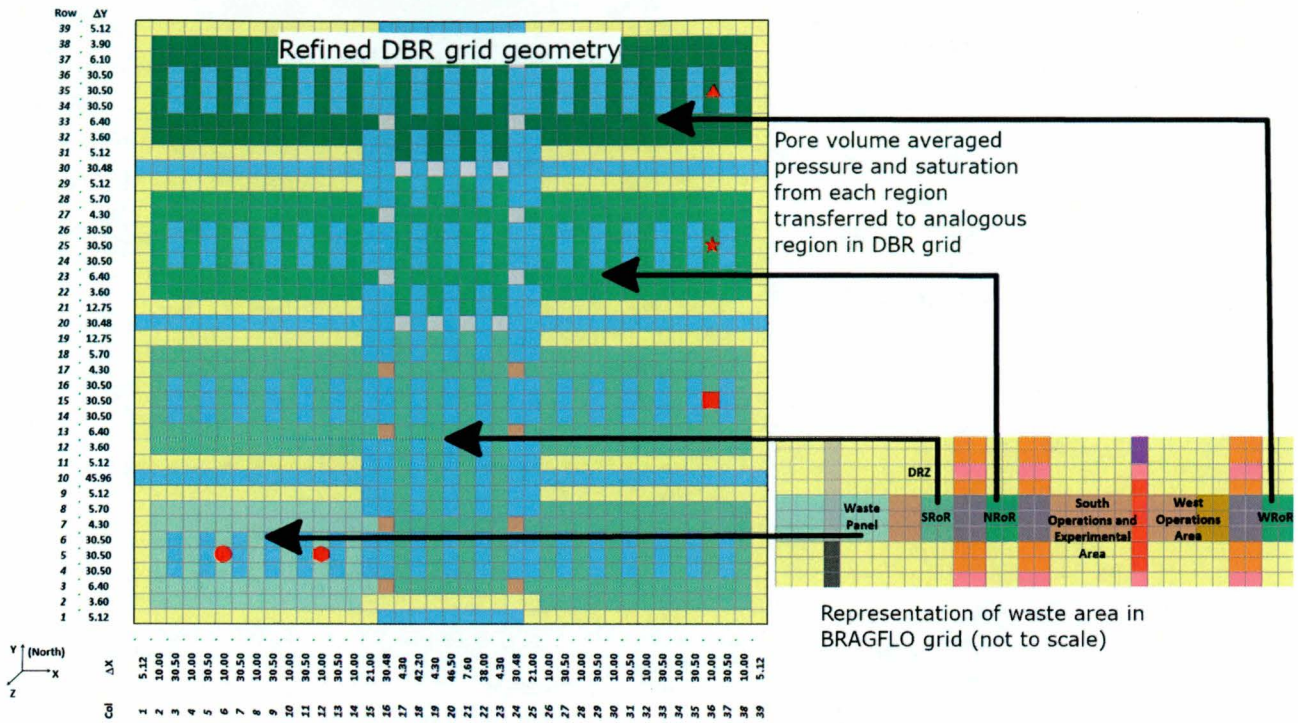


Figure 3: Regions used to transfer initial pressure and saturation from the BRAGFLO Salado grid to the DBR grid.

Information Only

3.0 DBR METHODOLOGY

This section provides an overview of the methodology used in the RPPCR DBR calculations, including the modeled scenarios and run control narrative.

3.1 Modeled Scenarios

In performing DBR calculations, five of the BRAGLFO Salado flow model scenarios, S1-BF to S5-BF, are used to set the initial conditions for the DBR calculations at the time of intrusion. As described by King (2023), the five BRAGFLO Salado flow scenarios capture the long-term behavior of the repository under three different conditions: undisturbed (E0); intersected by a borehole that continues down to a hypothetical pressurized brine reservoir below the repository (E1); and intersected by a borehole that does not intersect pressurized regions below the repository (E2). DBR calculations map the resulting BRAGFLO pressure and saturation conditions at a suite of intrusion times onto the DBR model grid and simulate flow to the intrusion. The scenarios and intrusion times used for the RPPCR, presented in Table 2, are the same as those used for the CRA-2019 PA. Note that the addition of the O intrusion location in the RPPCR results in a total of 104 combinations, or DBR simulations, for each parameter vector. In the CRA-2019, with only L, M and U intrusion locations, there were 78 DBR simulations per parameter vector.

Table 2 – DBR Scenarios

Scenario	Description
S1-DBR	Initially undisturbed repository (E0 conditions). Intrusion at the L, M, U, or O location at 100; 350; 1,000; 3,000; 5,000; or 10,000 years: 24 combinations.
S2-DBR	Initial E1 intrusion at 350 years followed by a second intrusion at the L, M, U, or O location at 550; 750; 2,000; 4,000; or 10,000 years: 20 combinations.
S3-DBR	Initial E1 intrusion at 1,000 years followed by a second intrusion at the L, M, U, or O location at 1,200; 1,400; 3,000; 5,000; or 10,000 years: 20 combinations.
S4-DBR	Initial E2 intrusion at 350 years followed by a second intrusion at the L, M, U, or O location at 550; 750; 2,000; 4,000; or 10,000 years: 20 combinations.
S5-DBR	Initial E2 intrusion at 1,000 years followed by a second intrusion at the L, M, U, or O location at 1,200; 1,400; 3,000; 5,000; or 10,000 years: 20 combinations.

3.2 Code Execution and Run Control

A flow diagram that illustrates the execution order for the DBR model is provided in Figure 4. A full description of the run control for the RPPCR analysis, including names and locations of input and output files, can be found in Long (2023).

Information Only

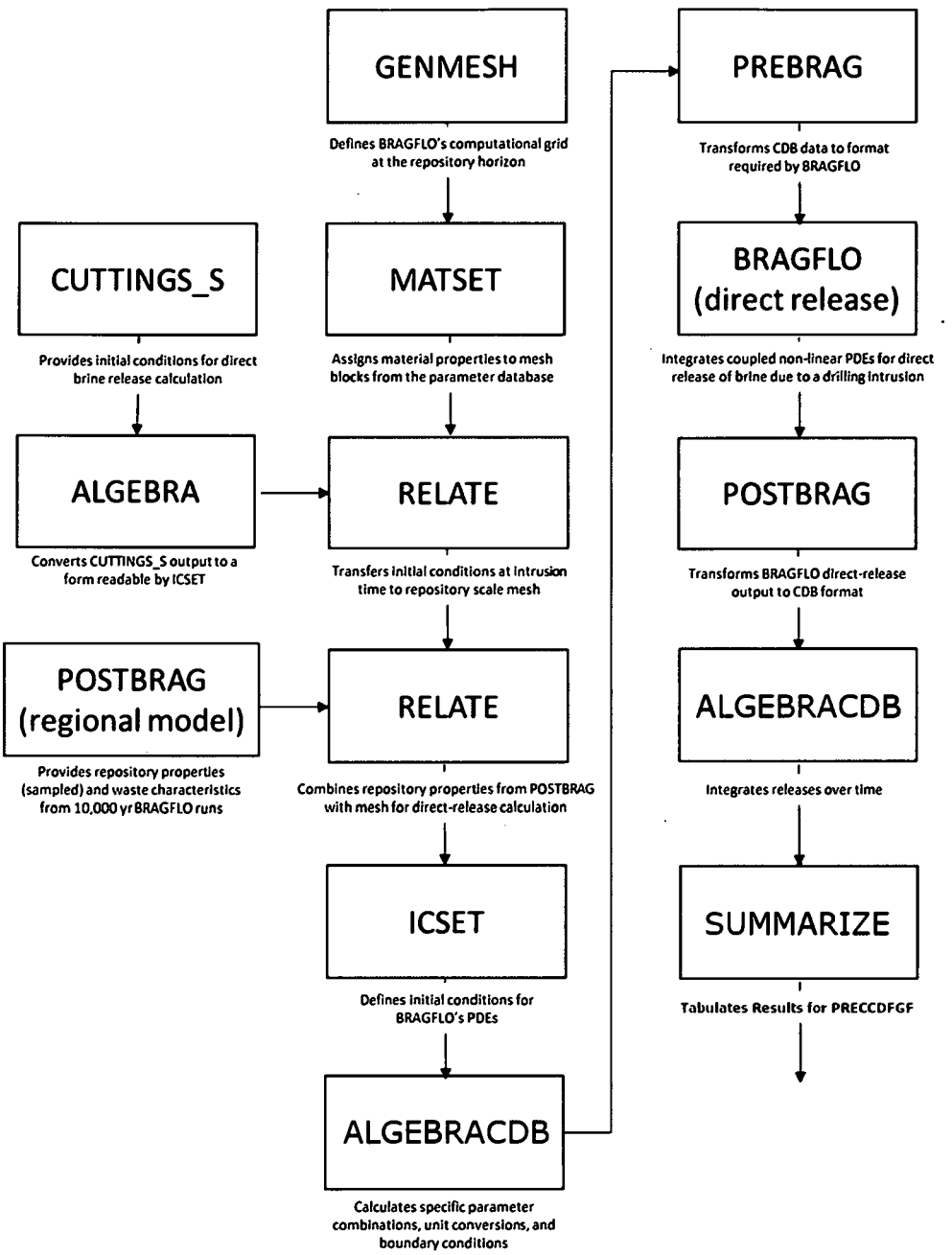


Figure 4: DBR run control diagram.

Information Only

4.0 RESULTS

The DBR calculation results for the RPPCR are presented in this section and compared to results from the CRA-2019 PA.

The analysis of the CRA-2019 DBR results is described in Bethune (2019) and will only be summarized herein as appropriate. Unless otherwise noted, results are summarized from all three replicates of 100 vectors each. Note that analysis name CRA-2019 is shortened to CRA19 in the tables and figures below.

Results from all scenarios are summarized below. Results are then further examined for scenarios S1-DBR, S2-DBR, and S4-DBR. Results from S3-DBR and S5-DBR are not examined individually because the only difference between them and S2-DBR and S4-DBR, respectively, is in the timing of drilling intrusions.

Summary statistics and plots were generated with Python, an open-source software package. The average DBR volume is calculated by the sum of DBR volumes divided by the total number of simulations. The DBR volume data were obtained from the output variable BRIN_REL, which is calculated in the ALGEBRACDB post-processing step and tabulated with PA code SUMMARIZE. For consistency with previous analyses, in calculating average non-zero DBR volumes and rates, non-zero volumes are defined as volumes that are greater than 10^{-7} m^3.

In addition to tables, many of the results are presented as boxplots, which graphically depict the distribution of the data by drawing boxes around the 25th (Q_{25}) and 75th (Q_{75}) percentiles of the distribution with a bisecting line at the median. The box whiskers extend out from the box to either an additional $1.5*(Q_{75} - Q_{25})$ or to the full range of the data, whichever is closer to the median. Datapoints outside of the whisker range are marked on the plot with black diamonds. The mean value is marked with a white square on top of the box and whisker plot. Note that intrusion time is treated categorically when used as an axis on the boxplots in this section.

4.1 Summary

Mean brine releases, fraction of simulations with non-zero releases, and mean of non-zero brine releases are summarized in Table 3. The number of non-zero brine releases is plotted in Figure 5 and Figure 6 by brine release volume, and the distribution of non-zero brine release volumes is plotted in Figure 7. Figure 8 shows the distribution of non-zero release volumes broken down by scenario, and Figure 9 shows the number of non-zero releases by scenario.[1]

Making an overall comparison of DBRs for the CRA-2019 and the RPPCR:

(i) The number of non-zero DBRs increased significantly for the RPPCR. Most of the increase came from scenarios S1-DBR, S4-DBR and S5-DBR, that is, from scenarios without a previous E1 intrusion (Figure 9).

(ii) The RPPCR saw small magnitude releases increase in frequency, while large magnitude releases decreased in frequency (Figures 5 and 6).

[1] Since releases from the O intrusion location have only a small effect on the RPPCR results shown in Figures 7-9, separate comparisons omitting the O intrusion are not provided.

Information Only

(iii) Mean, median and maximum non-zero release volumes all decreased for the RPPCR (Figure 7). Overall, the mean release volume decreased by a factor of about three (Table 3).

(iv) For the RPPCR, mean, median and maximum release volumes are comparable across the five intrusion scenarios (Figure 8). In the CRA-2019, scenarios S2-DBR and S3-DBR dominated these measures.

(v) For both the CRA-2019 and the RPPCR, the largest fraction of non-zero DBRs, and the largest mean non-zero release volume, occur at the L intrusion location; these measures decrease as the intrusion location moves to the north, that is, up dip (Table 3).

(vi) Releases from the O intrusion location, which was not included in the CRA-2019, contribute to RPPCR DBRs; however, O intrusion releases are less frequent and mean volumes are smaller compared to the L, M and U intrusion locations in the RPPCR (Table 3).

As described by King (2023), the RPPCR Salado flow results show an increase in mean and median brine pressures and, for scenarios without an E1 intrusion, an increase in brine saturation; these are effects that would tend to increase the number of non-zero DBRs. King (2023) also points out that maximum brine pressure is reduced in the RPPCR and, for scenarios with an E1 intrusion, there is a decrease in brine saturation; these are effects that will tend to reduce the largest DBR volumes.

Comparing RPPCR and CRA19 DBRs at individual intrusion locations (in Table 3, rows directly beneath the "All Scenarios" label), DBRs for the L and M intrusion locations follow the overall trend of a greater frequency of non-zero DBRs but with smaller mean release volumes in the RPPCR. In both analyses, DBRs from the L location have the greatest frequency and mean release volume. DBRs at the U intrusion location in the RPPCR increase both in frequency and in mean release volume; note though that mean release volumes at this location are very small in the CRA-2019. For the O intrusion location in the RPPCR, both the fraction of non-zero DBRs and the mean release volume are smaller than at other locations.

Scenarios with an E1 intrusion (S2-DBR and S3-DBR) have a similar frequency of non-zero DBRs in the CRA-2019 and the RPPCR; however, mean release volumes in the RPPCR are about one third those in the CRA-2019 (Table 3). The decrease in mean release volumes can be attributed to reduced brine saturation for scenarios with E1 intrusion, and to the smaller number of large magnitude releases (King, 2023).

Scenarios without an E1 intrusion (S1-DBR, S4-DBR and S5-DBR) saw the frequency of non-zero DBRs increase significantly in the RPPCR, while mean releases were reduced only somewhat (Table 3). The increase in non-zero DBR can be attributed to increased brine saturation for scenarios without an E1 intrusion, as well as an increase in mean pressure (King, 2023).

Information Only

Table 3 – DBR volume summary

Intrusion Location	Mean Brine Released (m^3)		Fraction of Simulations with Non-Zero Releases		Mean of Non-Zero Brine Releases (m^3)	
	CRA19	RPPCR	CRA19	RPPCR	CRA19	RPPCR
S1-DBR	**0.26**	**0.58**	**2.54%**	**9.58%**	**10.11**	**6.03**
L	0.70	1.51	5.44%	15.67%	12.87	9.66
M	0.07	0.34	1.17%	7.22%	5.62	4.74
U	0.00	0.34	1.00%	8.89%	0.30	3.88
O	-	0.11	-	6.56%	-	1.66
S2-DBR	**8.29**	**2.18**	**47.22%**	**37.90%**	**17.55**	**5.76**
L	15.64	5.46	73.53%	74.27%	21.27	7.35
M	9.21	2.56	66.07%	55.40%	13.94	4.61
U	0.00	0.57	2.07%	14.40%	0.15	3.99
O	-	0.14	-	7.53%	-	1.88
S3-DBR	**5.23**	**1.43**	**40.44%**	**33.22%**	**12.94**	**4.31**
L	10.83	3.73	66.60%	66.33%	16.27	5.63
M	4.86	1.18	52.93%	40.60%	9.19	2.9
U	0.00	0.61	1.80%	15.40%	0.22	3.98
O	-	0.2	-	10.53%	-	1.92
S4-DBR	**0.07**	**0.78**	**1.04%**	**12.72%**	**7.14**	**6.11**
L	0.22	1.84	2.27%	19.40%	9.83	9.51
M	0.00	0.66	0.40%	11.67%	0.18	5.65
U	0.00	0.47	0.47%	12.33%	0.01	3.82
O	-	0.14	-	7.47%	-	1.81
S5-DBR	**0.12**	**1.02**	**1.62%**	**14.88%**	**7.70**	**6.84**
L	0.36	2.43	3.60%	22.33%	10.10	10.86
M	0.01	0.81	0.80%	12.87%	1.38	6.27
U	0.00	0.64	0.47%	13.93%	0.01	4.58
O	-	0.2	-	10.40%	-	1.96
All Scenarios						
L	**5.37**	**2.94**	**29.33%**	**38.68%**	**18.29**	**7.6**
M	**2.72**	**1.08**	**23.38%**	**24.85%**	**11.65**	**4.34**
U	**0.00**	**0.52**	**1.15%**	**12.83%**	**0.18**	**4.06**
O	**-**	**0.16**	**-**	**8.42%**	**-**	**1.86**
L, M, and U	**2.70**	**1.51**	**17.96%**	**25.45%**	**15.02**	**5.94**
ALL	**2.70**	**1.17**	**17.96%**	**21.20%**	**15.02**	**5.54**

Information Only

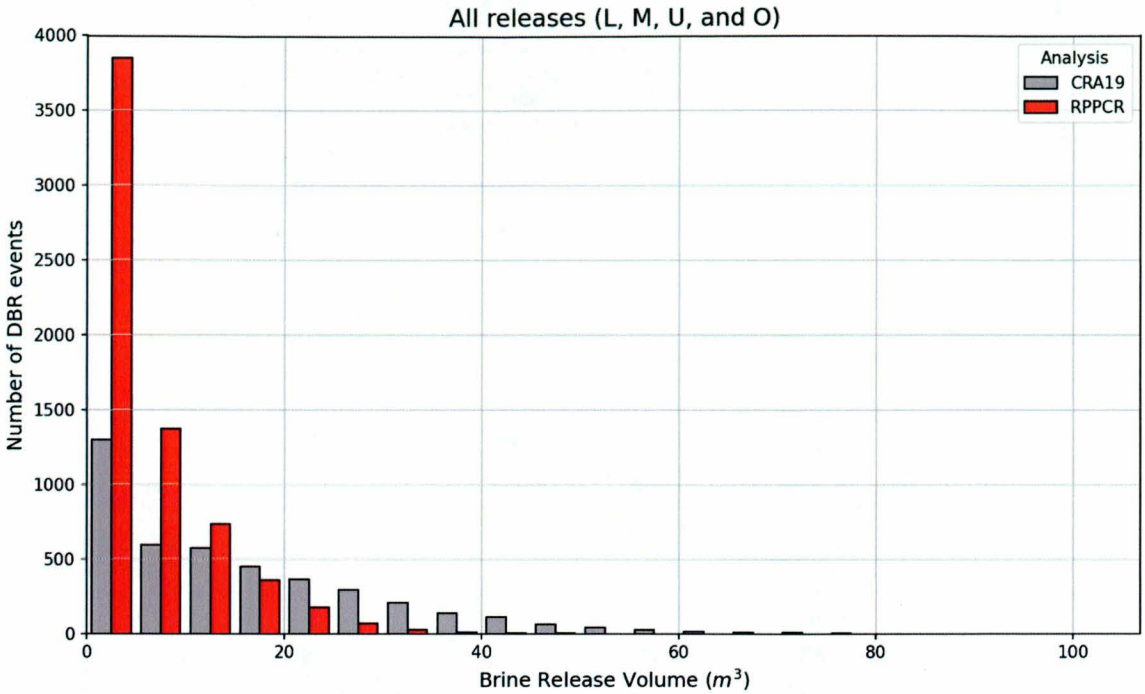


Figure 5: Release volume frequency, all non-zero releases

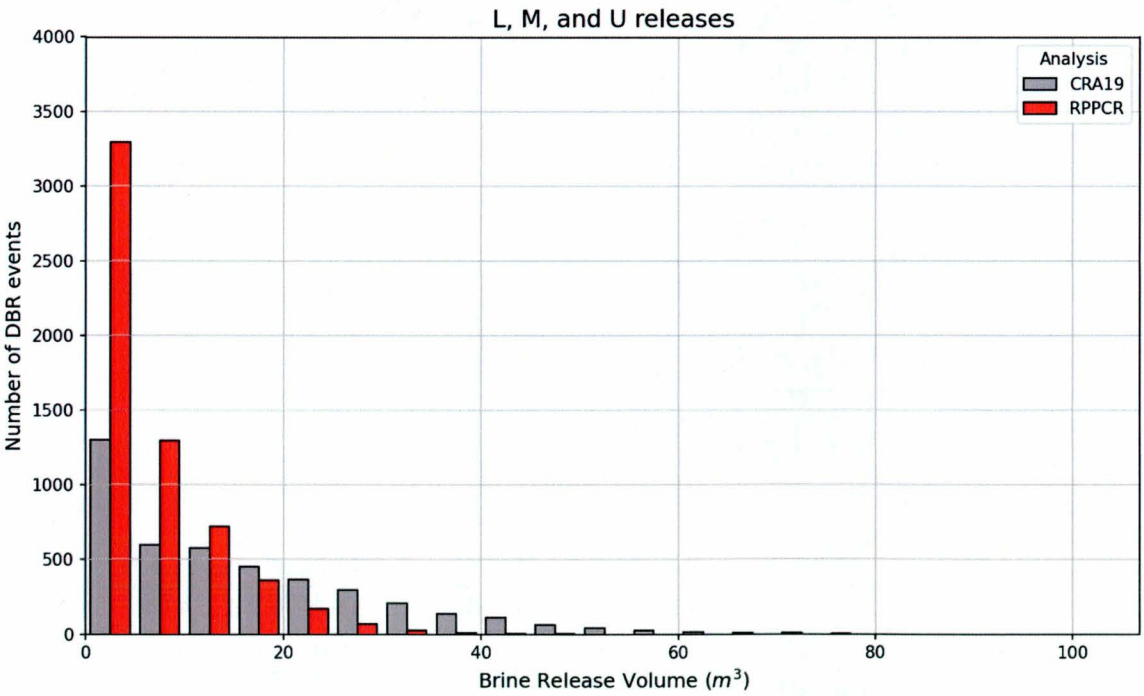


Figure 6: Release volume frequency, L, M, and U non-zero releases only

Information Only

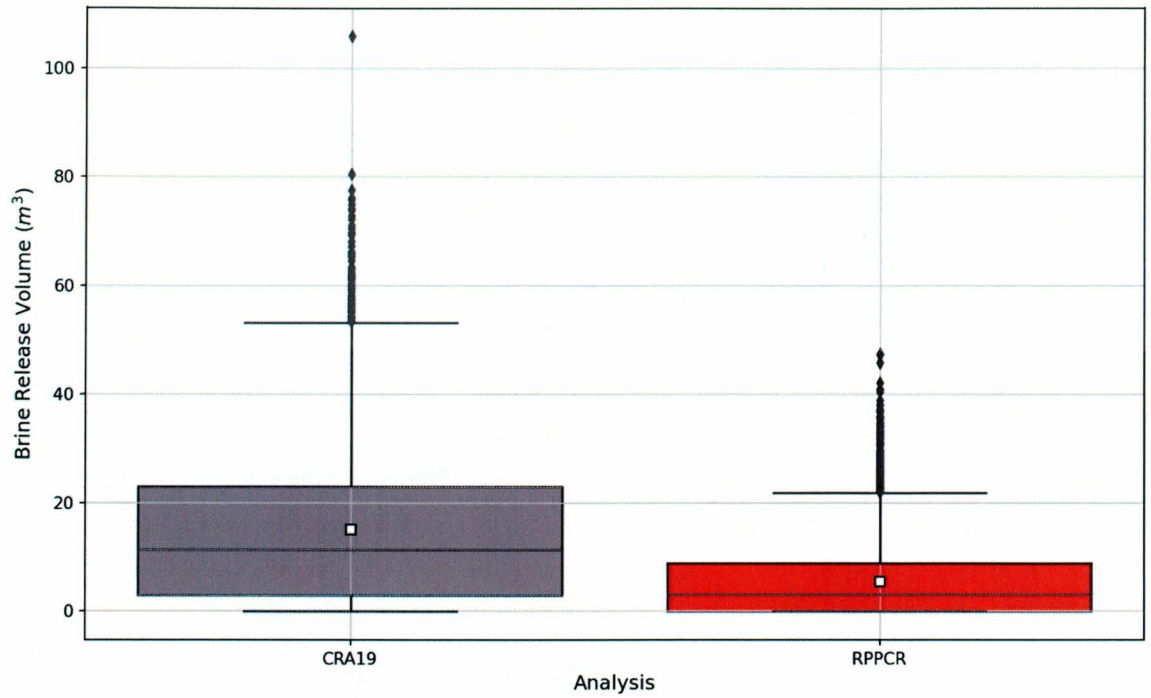


Figure 7: Release volumes, all non-zero releases

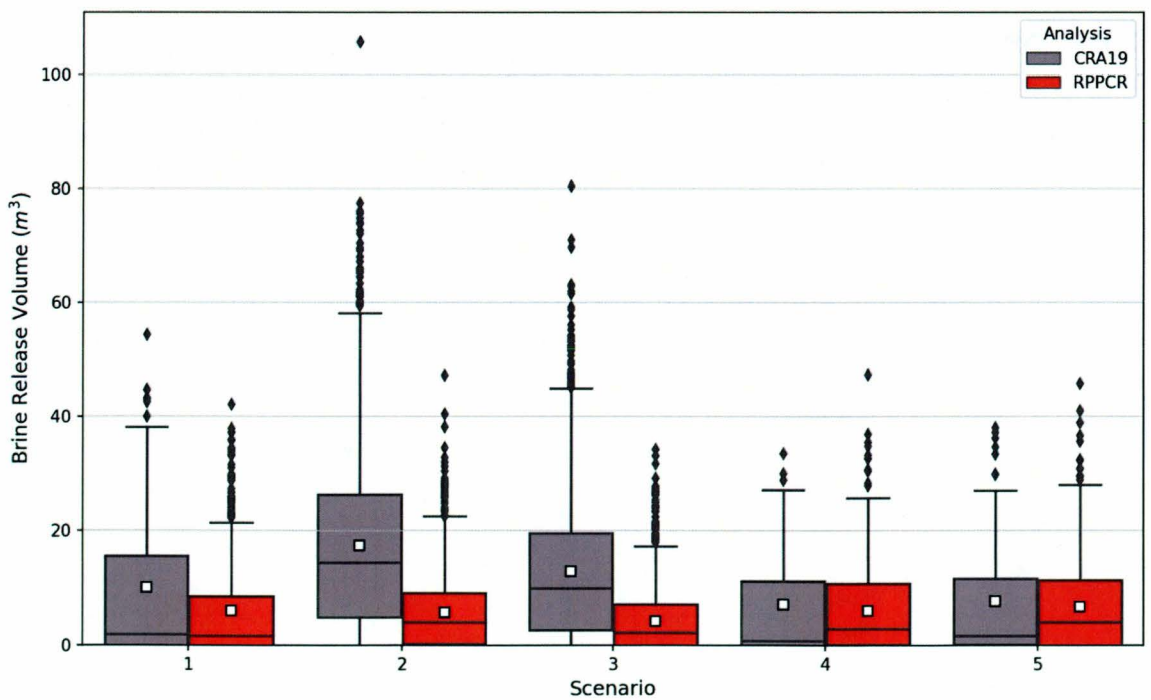


Figure 8: Release volumes by scenario, all non-zero releases

Information Only

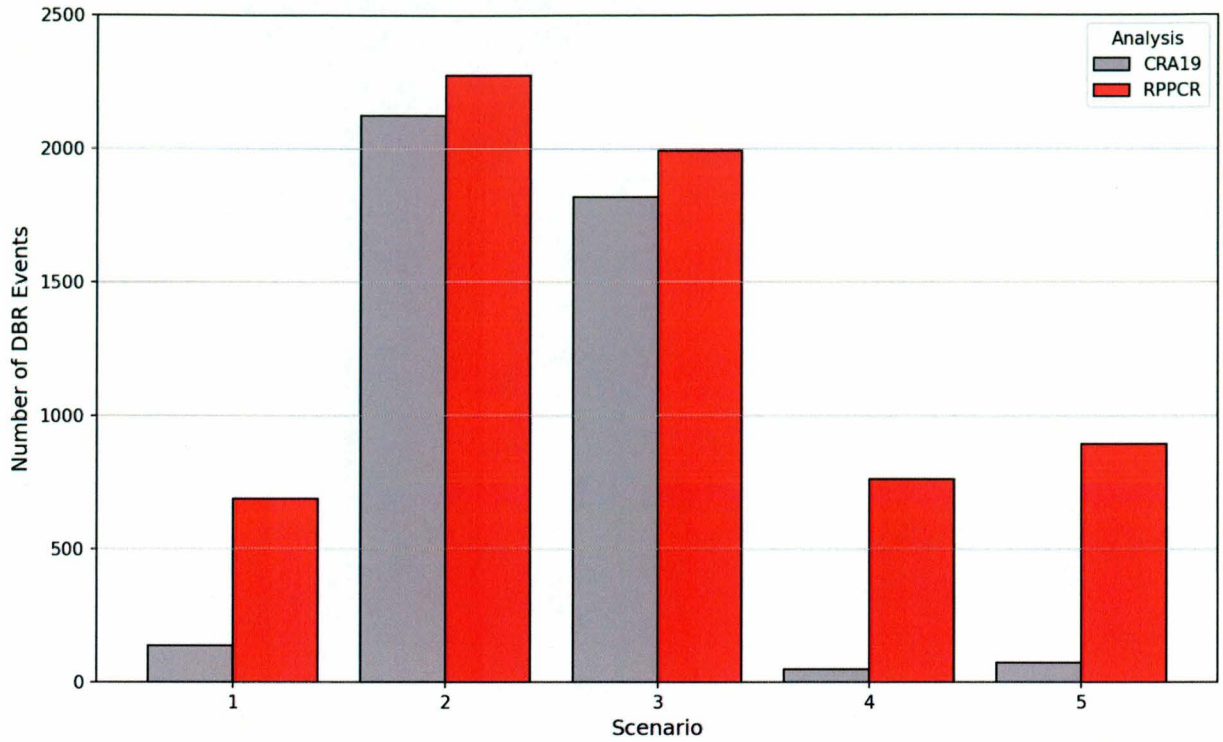


Figure 9: Number of non-zero DBR events by scenario

4.2 S1-DBR

The S1-DBR scenario models DBRs resulting from an intrusion into a previously undisturbed repository (Table 2). Mean brine release volume, fraction of simulations with non-zero releases, and mean volume from non-zero releases are summarized in Table 4. Non-zero release volumes for S1-DBR intrusions are plotted in Figure 10, grouped by intrusion location and time.

Compared to the CRA-2019, the S1-DBR fraction of simulations with non-zero releases increased significantly for the RPPCR, while the mean non-zero release volumes remained comparable (Table 4). The results are consistent with other scenarios that do not involve an E1 intrusion.

Information Only

Table 4 – S1-DBR volume summary

Intrusion Location and Time (yr)	Mean Brine Released (m^3)		Fraction of Simulations with Non-Zero Releases		Mean of Non-Zero Brine Releases (m^3)	
	CRA19	RPPCR	CRA19	RPPCR	CRA19	RPPCR
L	**0.70**	**1.51**	**5.44%**	**15.67%**	**12.87**	**9.66**
100	0.00	0	0.00%	0.00%	-	-
350	0.00	0.11	0.00%	3.00%	-	3.67
1,000	0.11	2.03	2.00%	21.67%	5.64	9.37
3,000	1.26	3.01	9.00%	23.00%	14.05	13.1
5,000	1.39	2.31	10.00%	23.33%	13.95	9.91
10,000	1.43	1.61	11.67%	23.00%	12.28	7.01
M	**0.07**	**0.34**	**1.17%**	**7.22%**	**5.62**	**4.74**
100	0.00	0	0.00%	0.00%	-	-
350	0.00	0.07	0.00%	3.00%	-	2.36
1,000	0.06	1.15	0.67%	18.00%	9.51	6.39
3,000	0.16	0.46	2.33%	10.67%	6.73	4.3
5,000	0.13	0.27	1.67%	6.33%	8.05	4.2
10,000	0.04	0.11	2.33%	5.33%	1.67	2.07
U	**0.00**	**0.34**	**1.00%**	**8.89%**	**0.30**	**3.88**
100	0.00	0	0.00%	0.00%	-	-
350	0.00	0.02	0.00%	1.33%	-	1.47
1,000	0.00	0.99	0.00%	17.33%	-	5.7
3,000	0.01	0.59	2.00%	15.00%	0.46	3.94
5,000	0.01	0.32	2.00%	9.67%	0.33	3.34
10,000	0.00	0.15	2.00%	10.00%	0.10	1.47
O	-	**0.11**	-	**6.56%**	-	**1.66**
100	-	0	-	0.00%	-	-
350	-	0.02	-	0.67%	-	3.42
1,000	-	0.28	-	8.33%	-	3.37
3,000	-	0.23	-	12.00%	-	1.9
5,000	-	0.06	-	10.67%	-	0.61
10,000	-	0.06	-	7.67%	-	0.76
S1-DBR	**0.26**	**0.58**	**2.54%**	**9.58%**	**10.11**	**6.03**

Information Only

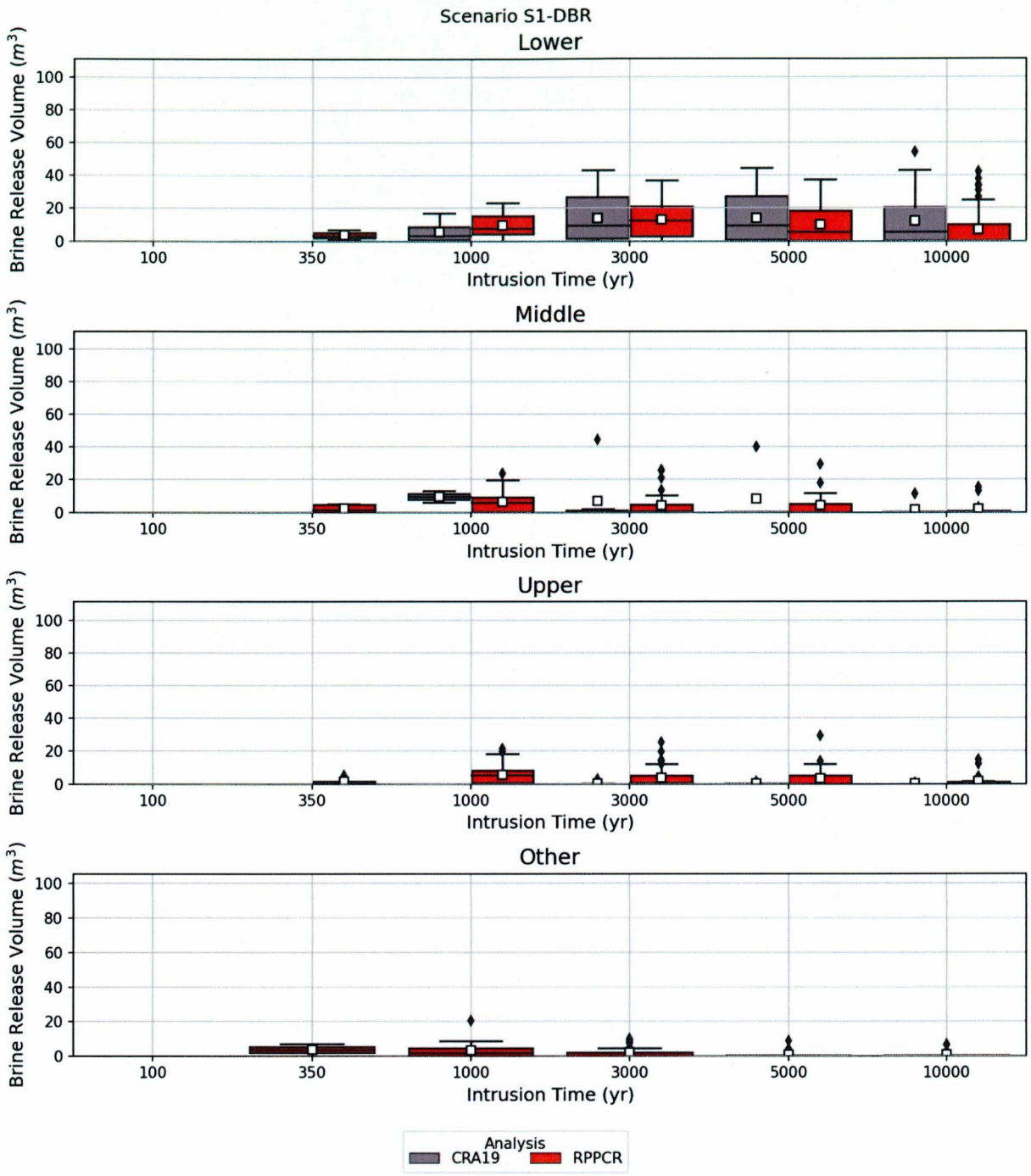


Figure 10: S1-DBR release volumes, all non-zero releases

Information Only

4.3 S2-DBR

The S2-DBR scenario models DBRs resulting from a repository that has been previously intruded by a wellbore that also intersected a pressurized brine pocket in the Castile formation (Table 2). Initial conditions for this scenario are explored in Section 5.1. The RPPCR S2-DBR releases are summarized in Table 5, with the CRA19 values shown for comparison. Release volumes for all S2-DBR intrusions are plotted in Figure 11, grouped by intrusion location and time.

For the L and M intrusion locations, the fraction of non-zero releases stayed about the same for the RPPCR compared to the CRA-2019; however, mean releases fell by a factor of about 3. The situation is somewhat different at the U intrusion location, where both the frequency of non-zero releases and mean releases increase in the RPPCR. Note however that releases associated with the U intrusion are very small in the CRA-2019 and that U releases in the RPPCR, though increased over the CRA-2019, are still fewer in number (by a factor of 4 or more) than releases at the L and M intrusion locations.

The overall reduction in RPPCR DBRs in the S2-DBR scenario is attributed to reduced brine saturation where E1 intrusions are involved, as mentioned in Section 4.1. Fewer large magnitude releases due to reduced maximum pressure contribute to the overall reduction. Increased DBRs at the U intrusion location are consistent with an increase in small magnitude releases in the RPPCR.

Information Only

Table 5 – S2-DBR volume summary

Intrusion Location and Time (yr)	Mean Brine Released (m^3)		Fraction of Simulations with Non-Zero Releases		Mean of Non-Zero Brine Releases (m^3)	
	CRA19	RPPCR	CRA19	RPPCR	CRA19	RPPCR
L	**15.64**	**5.46**	**73.53%**	**74.27%**	**21.27**	**7.35**
550	9.45	3.91	82.33%	91.33%	11.48	4.28
750	15.87	6.17	90.67%	89.00%	17.50	6.94
2000	20.31	7.48	75.67%	73.67%	26.83	10.15
4000	18.19	5.44	64.33%	63.00%	28.27	8.63
10000	14.41	4.3	54.67%	54.33%	26.35	7.92
M	**9.21**	**2.56**	**66.07%**	**55.40%**	**13.94**	**4.61**
550	10.86	2.71	81.00%	85.33%	13.40	3.18
750	13.13	3.49	89.33%	74.67%	14.70	4.68
2000	12.18	3.63	69.67%	54.67%	17.48	6.63
4000	7.23	1.88	53.00%	35.67%	13.64	5.26
10000	2.66	1.07	37.33%	26.67%	7.12	4.01
U	**0.00**	**0.57**	**2.07%**	**14.40%**	**0.15**	**3.99**
550	0.00	0.32	0.00%	10.67%	-	3.03
750	0.00	0.68	0.00%	16.67%	-	4.1
2000	0.00	1.31	3.00%	18.67%	0.09	7.03
4000	0.01	0.36	4.67%	13.67%	0.25	2.66
10000	0.00	0.19	2.67%	12.33%	0.04	1.53
O	-	**0.14**	-	**7.53%**	-	**1.88**
550	-	0.06	-	2.33%	-	2.62
750	-	0.14	-	5.33%	-	2.54
2000	-	0.31	-	11.33%	-	2.7
4000	-	0.13	-	10.67%	-	1.25
10000	-	0.07	-	8.00%	-	0.91
S2-DBR	**8.29**	**2.18**	**47.22%**	**37.90%**	**17.55**	**5.76**

Information Only

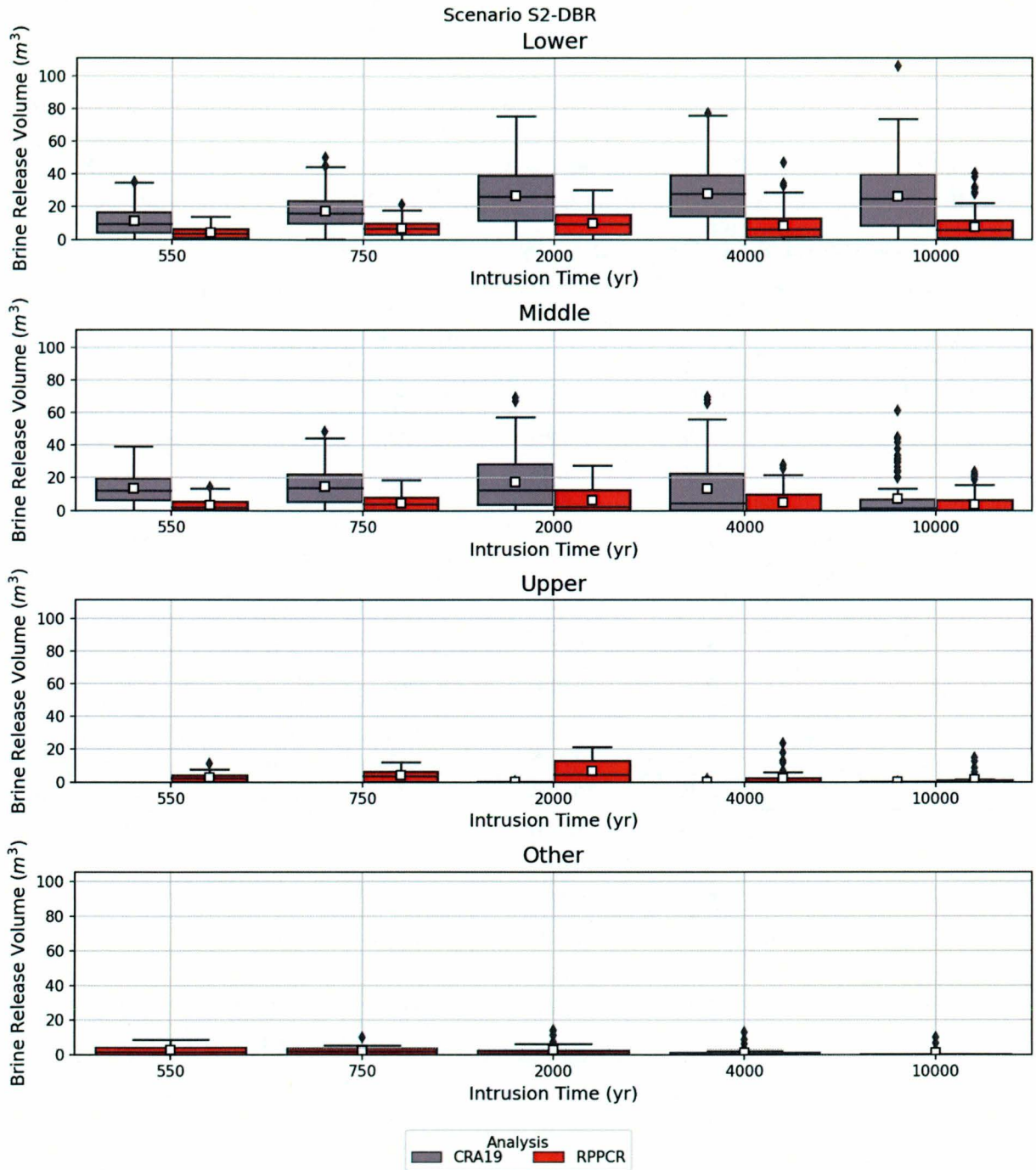


Figure 11: S2-DBR release volumes, all non-zero releases

4.4 S4-DBR

The S4-DBR scenario models DBRs resulting from a repository that had been previously intruded by a wellbore that did not intersect a pressurized brine pocket in the Castile formation (Table 2).

Information Only

RPPCR S4-DBR release volumes are summarized in Table 6, with CRA19 values for comparison. Release volumes for all S4-DBR intrusions are plotted in Figure 12, grouped by intrusion location and time.

RPPCR S4-DBRs follow the trend of other scenarios without an E1 intrusion, namely a large increase in non-zero DBRs compared to the CRA-2019, and – taking an overall comparison – a mean non-zero volume similar to that in the CRA-2019. Note that RPPCR releases at the M and U intrusion locations are significant; in the CRA-2019, DBRs at these locations were negligible.

Table 6 – S4-DBR volume summary

Intrusion Location and Time (yr)	Mean Brine Released (m^3)		Fraction of Simulations with Non-Zero Releases		Mean of Non-Zero Brine Releases (m^3)	
	CRA19	RPPCR	CRA19	RPPCR	CRA19	RPPCR
L	**0.22**	**1.84**	**2.27%**	**19.40%**	**9.83**	**9.51**
550	0.00	0.7	0.00%	12.67%	-	5.54
750	0.00	1.24	0.00%	18.33%	-	6.75
2000	0.25	2.81	2.33%	22.33%	10.75	12.57
4000	0.42	2.62	4.67%	20.67%	8.93	12.7
10000	0.45	1.85	4.33%	23.00%	10.30	8.05
M	**0.00**	**0.66**	**0.40%**	**11.67%**	**0.18**	**5.65**
550	0.00	0.55	0.00%	10.33%	-	5.29
750	0.00	0.94	0.00%	15.00%	-	6.23
2000	0.00	1.08	0.33%	15.67%	0.00	6.88
4000	0.00	0.41	0.67%	9.33%	0.43	4.43
10000	0.00	0.32	1.00%	8.00%	0.08	4.01
U	**0.00**	**0.47**	**0.47%**	**12.33%**	**0.01**	**3.82**
550	0.00	0.27	0.00%	7.67%	-	3.55
750	0.00	0.61	0.00%	14.33%	-	4.22
2000	0.00	1.08	0.00%	17.33%	-	6.24
4000	0.00	0.27	1.67%	11.33%	0.00	2.37
10000	0.00	0.13	0.67%	11.00%	0.04	1.17
O	-	**0.14**	-	**7.47%**	-	**1.81**
550	-	0.06	-	2.33%	-	2.61
750	-	0.13	-	5.33%	-	2.53
2000	-	0.29	-	11.00%	-	2.67
4000	-	0.13	-	10.33%	-	1.26
10000	-	0.06	-	8.33%	-	0.68
S4-DBR	**0.07**	**0.78**	**1.04%**	**12.72%**	**7.14**	**6.11**

Information Only

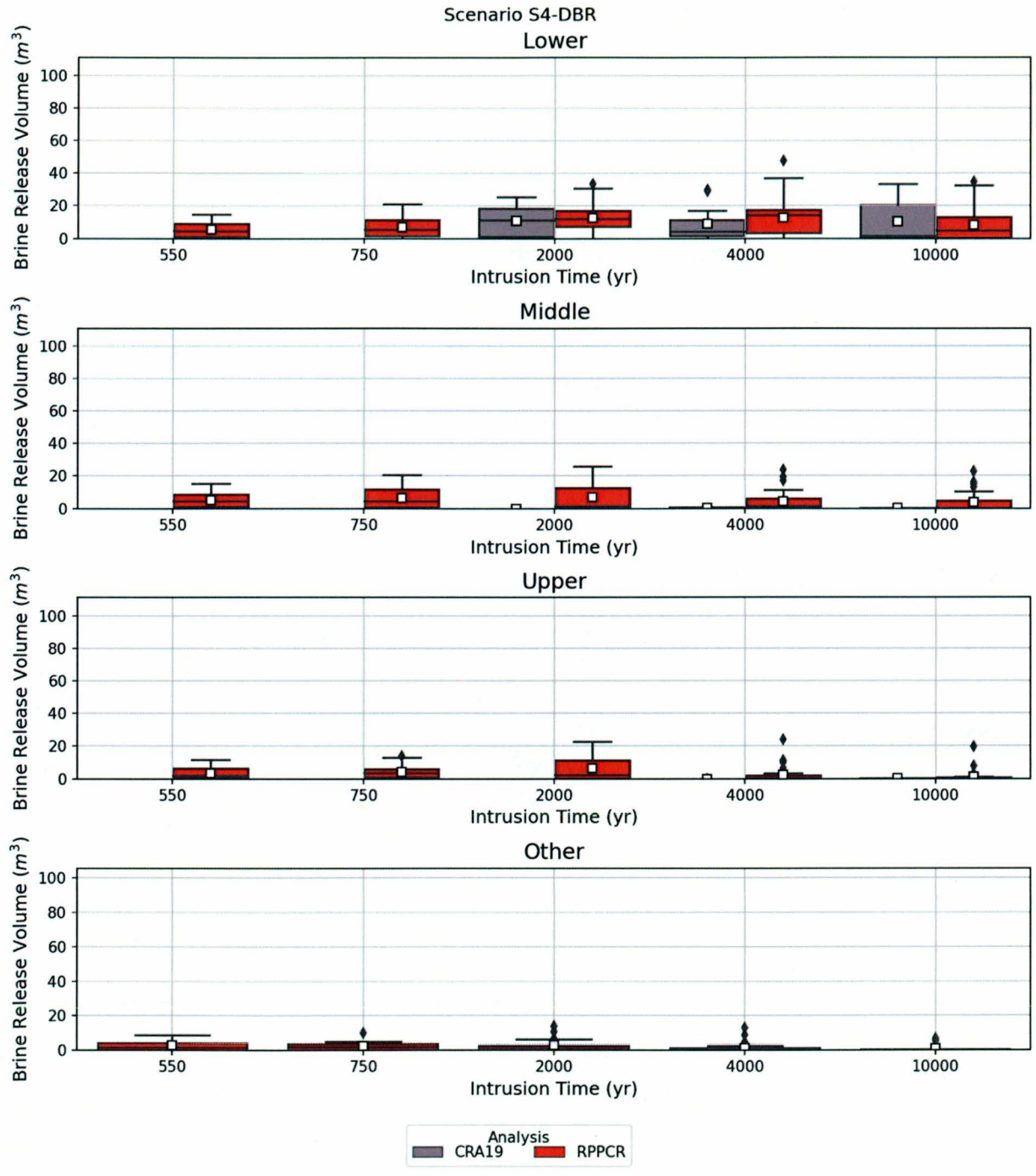


Figure 12: S4-DBR releases volumes, all non-zero releases

Information Only

4.5 Maximum Releases

The ten largest brine release volumes for the RPPCR and CRA19 are shown in Table 7. The ten largest DBR volumes decreased significantly in the RPPCR compared to the CRA-2019. Note that the absolute largest release volumes for each analysis do not necessarily come from simulations with the highest saturation or pressure. From the table:

(i) For the RPPCR, the ten largest DBR volumes decreased to about one half the magnitudes seen in the CRA-2019.

(ii) All but one of the largest RPPCR DBR volumes came from the L intrusion location. All of the CRA-2019 largest volumes came from the L intrusion.

(iii) For the RPPCR, four of the largest volumes came from scenarios with a previous E2 intrusion; three came from scenarios with a previous E1 intrusion; and three were from scenarios with no previous intrusion. For comparison, all of the CRA-2019 largest volumes were associated with scenarios that had a previous E1 intrusion.

(iv) For the RPPCR, one vector was associated with the three top releases, and five out of the top ten. Similarly, one vector was associated with the top three releases in the CRA-2019.

Table 7 – Largest DBR volumes by analysis

Analysis	Rank	Replicate	Scenario	Time (yr)	Vector	Location	Release (m^3)	Pressure (MPa)	Saturation (-)
RPPCR	1	1	4	4000	28	L	47.38	15.35	0.948
RPPCR	2	1	2	4000	28	L	47.25	15.34	0.948
RPPCR	3	1	5	3000	28	L	45.74	15.49	0.948
RPPCR	4	1	1	10000	8	L	42.11	15.38	0.864
RPPCR	5	1	5	5000	28	L	40.94	14.56	0.948
RPPCR	6	1	2	10000	6	L	40.45	15.3	0.991
RPPCR	7	1	5	5000	28	M	38.85	14.52	0.819
RPPCR	8	3	2	10000	15	L	38.12	15.32	0.996
RPPCR	9	2	1	10000	63	L	37.92	15.27	0.937
RPPCR	10	2	1	5000	78	L	37.21	15.33	0.991
						Mean	**41.6**	**15.19**	**0.939**
CRA19	1	3	2	10000	99	L	105.79	17.18	0.902
CRA19	2	3	3	10000	99	L	80.46	16.82	0.842
CRA19	3	3	2	4000	99	L	77.44	16.59	0.961
CRA19	4	2	2	4000	1	L	76.07	14.40	0.991
CRA19	5	3	2	2000	94	L	75.67	16.06	0.974
CRA19	6	3	2	2000	81	L	74.78	15.60	0.815
CRA19	7	3	2	4000	94	L	74.05	15.82	0.975
CRA19	8	2	2	10000	78	L	73.82	14.65	0.991
CRA19	9	2	2	4000	78	L	72.72	14.60	0.851
CRA19	10	3	2	10000	15	L	72.13	15.67	0.997
						Mean	**78.29**	**15.74**	**0.930**

Information Only

5.0 DRIVERS AND CORRELATIONS

Volume-averaged brine pressure and brine saturation in the intruded panel are the two most important variables that control DBR volumes (Clayton et al., 2008). In this section, brine pressure and saturation initial conditions for the DBR simulations are summarized and compared for the RPPCR and CRA-2019 analyses. For a discussion of the modeling setup that produces the initial conditions, and a more comprehensive analysis of those results, see the RPPCR Salado flow analysis report (King, 2023).

As has been done for previous DBR analysis reports (e.g., Bethune, 2019), sensitivity of DBR volumes to brine pressure and saturation initial conditions will also be qualitatively examined. Pressure and saturation values were extracted from the ALGEBRACDB output files generated as a preprocessing step for the DBR input (Figure 4). Pressure and saturation values were extracted from the intruded region, and so represent the pressure and saturation conditions encountered by the intrusion.

Also consistent with previous reports (e.g., Stoelzel and O'Brien, 1996), only scenario S2-DBR will be discussed below in the presentation of initial conditions and the sensitivity analysis. Scenario S2-DBR has the greatest number of non-zero releases in both the CRA-2019 and the RPPCR (Figure 9).

Because intrusions at the L location had previously produced the majority of DBRs, they were the only intrusions examined in the sensitivity studies of previous DBR analysis packages (e.g., Stoelzel and O'Brien 1996). With the abandonment of panel closure systems in the south of the repository, M intrusion locations from CRA-2019 were also included in the CRA-2019 DBR analysis (Bethune, 2019). For the RPPCR analysis, all four intrusion locations will be examined for comparison.

The sensitivity of DBRs to those parameters that most influence brine pressure and saturation in the RPPCR Salado Flow simulations is illustrated in an appendix at the end of this report.

5.1 Initial Conditions Summary

RPPCR DBR mean initial conditions are presented in Table 8 with CRA-2019 values for comparison. Boxplots of initial pressure and saturation are shown in Figure 13 and Figure 14.

Mean and median initial brine pressures for L, M and U intrusion locations increased in the RPPCR compared to the CRA-2019; the increases are seen at all intrusion times. Maximum initial brine pressures occur at later intrusion times and are greatest in the CRA-2019. Note also that initial brine pressures tend to increase with intrusion time for both the RPPCR and the CRA-2019.

For the L and M locations, most intrusions encounter pressure conditions above the 8 MPa threshold for a DBR – this is true for both the RPPCR and the CRA-2019. For the U location, more intrusions encounter the 8 MPa threshold in the RPPCR than in the CRA-2019. Mean pressures at the O location in the RPPCR exceed the 8 MPa threshold only at the year 10,000 intrusion time.

Brine saturations in the RPPCR decreased at the L and M locations compared to the CRA-2019 – both means and medians for all intrusion times (Figure 14). Intrusions at the L location also encountered a wider range of brine saturation values in the RPPCR, as did intrusions at earlier

Information Only

times for the M location. For both analyses, saturation tends to decrease with time at the L and M locations.

At the U location, mean brine saturations increased in the RPPCR over the CRA-2019; however, saturation levels are low for both analyses. Saturations are also low at the O location in the RPPCR. (Although not clear in Figure 14, median brine saturations are less than or equal to 0.02 at the U and O locations for all intrusion times in both analyses.)

Table 8 – S2-DBR mean initial conditions.

Intrusion Location and Time (yr)	Brine Pressure (MPa)		Brine Saturation (-)	
	CRA19	RPPCR	CRA19	RPPCR
L	**10.2**	**11.4**	**0.87**	**0.64**
550	9.2	10	0.89	0.77
750	10.2	11.4	0.9	0.75
2000	10.9	12.5	0.87	0.64
4000	10.6	12	0.84	0.51
10000	10	10.8	0.83	0.52
M	**10.1**	**11.3**	**0.67**	**0.39**
550	9.1	10	0.79	0.61
750	10.1	11.4	0.78	0.57
2000	10.9	12.5	0.68	0.4
4000	10.6	12	0.56	0.23
10000	10	10.8	0.52	0.17
U	**6.2**	**8.5**	**0.05**	**0.14**
550	2.4	5	0.07	0.2
750	3.4	6.5	0.07	0.18
2000	7.1	9.9	0.05	0.14
4000	8.8	10.7	0.04	0.09
10000	9.6	10.5	0.03	0.08
O	-	**5.5**	-	**0.11**
550	-	3	-	0.17
750	-	3.5	-	0.16
2000	-	5.3	-	0.11
4000	-	6.9	-	0.07
10000	-	8.8	-	0.06
S2-DBR	**8.9**	**9.2**	**0.53**	**0.32**

Information Only

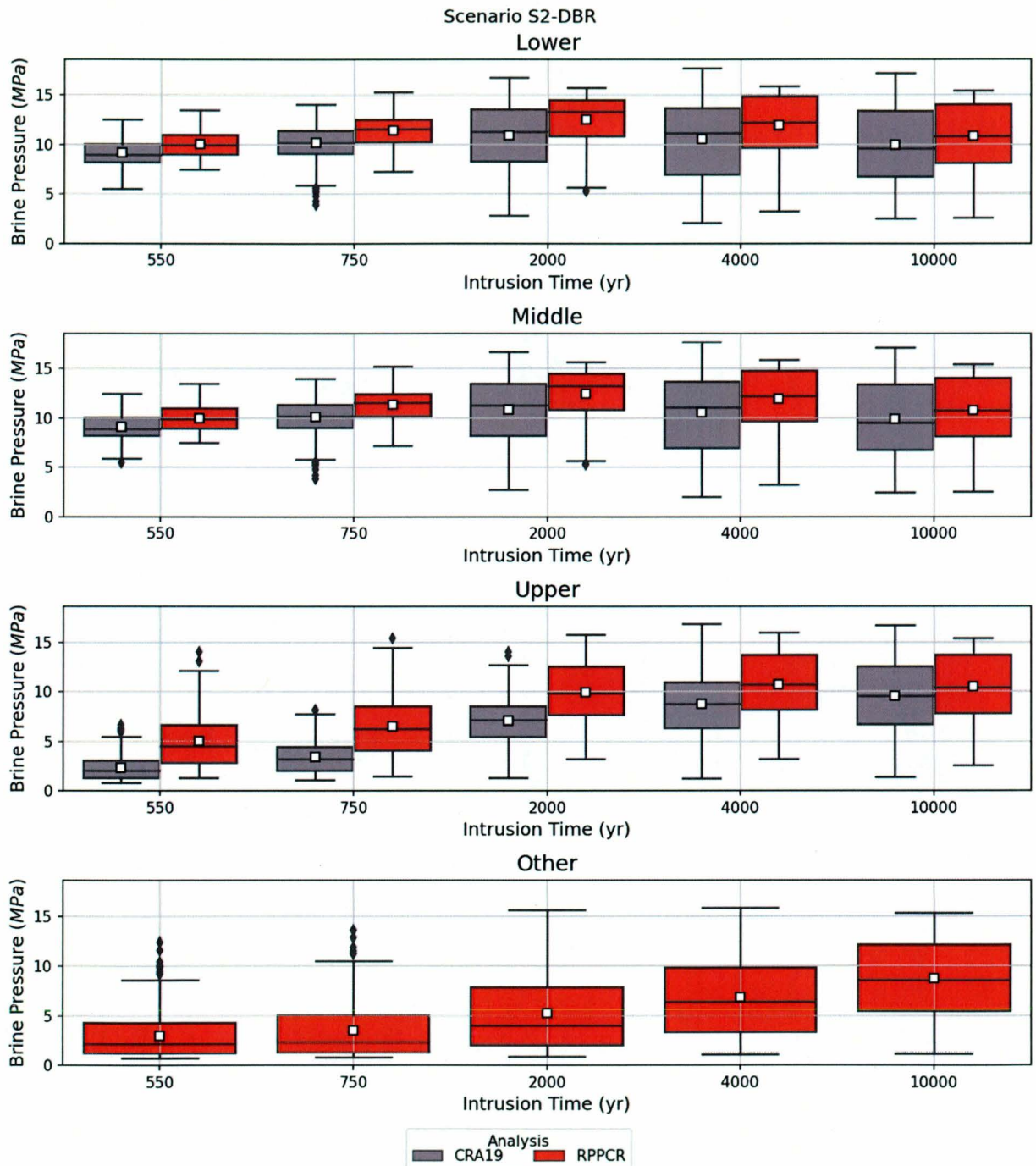


Figure 13: S2-DBR brine pressure, all intrusions.

Information Only

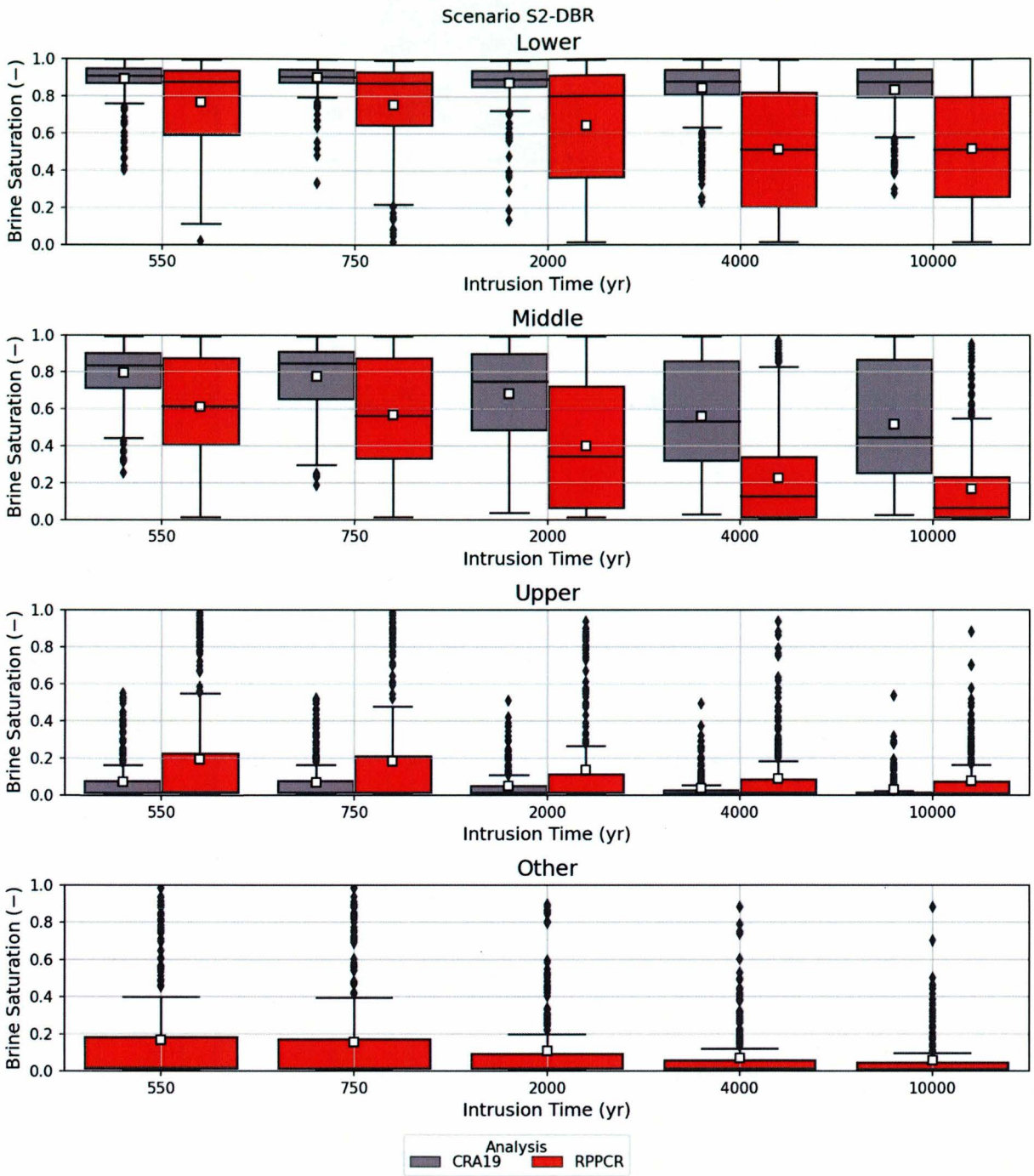


Figure 14: S2-DBR brine saturation, all intrusions

Information Only

5.2 Correlation and Sensitivity to Initial Conditions

Scatter plots were created to visualize the correlation and sensitivity of RPPCR DBR volume to initial panel pressure and saturation (Figure 15 and Figure 16, respectively) with the CRA-2019 plotted separately for comparison. As was done in previous DBR analysis reports, saturation is plotted as mobile brine saturation, calculated as brine saturation less the residual brine saturation (Stoelzel and O'Brien, 1996). Regression statistics were calculated with the python SciPy[2] statistics package, and the line of best fit plotted over the data. Simulations with zero releases were not plotted or included in the regression analysis.

Each simulation was categorized into flow regimes from the ratio of relative permeabilities of brine and gas, as is done in the ALGEBRACDB preprocessing step to calculate flowing bottom hole pressure (Equation 1 and Stoelzel and O'Brien, 1996). Simulations were categorized as "all brine" if the gas relative permeability is zero (equivalently, the gas saturation is the residual gas saturation), "brine dominated" if the gas relative permeability is lower than the brine relative permeability, and "gas dominated" if the gas relative permeability is higher than the brine relative permeability. Because flow regime is a function of both brine saturations and residual brine saturation, the same brine saturation can be categorized into multiple flow regimes (Figure 17 and Figure 18).

For the CRA-2019, Figure 15 (top) shows brine pressure has the strongest correlation with brine release volume when the panel is fully brine saturated, that is, the all-brine flow regime. (Here, strength of correlation is measured by the coefficient of correlation, reported as "r^2" in the figure.) When the panel is under a brine dominated flow regime, the correlation is slightly weaker. When the flow regime is gas dominated, brine pressure has little correlation with release volume.

For the RPPCR, gas relative permeability never reaches zero and consequently there is no all brine flow regime: Figure 15 (bottom) shows brine dominated and gas dominated flow regimes only for the RPPCR.[3] Of these, initial brine pressure has the strongest correlation with brine release volume in the brine dominated regime. When the RPPCR flow regime is gas dominated there is little correlation with release volume, as was the case for the CRA-2019. Note also that DBR volumes are much less sensitive to pressure in the RPPCR: the slope of the straight line fit in the RPPCR brine dominated flow regime is much less than either the all brine or the brine dominated line slopes in the CRA-2019.

Figure 16 shows brine saturation has the strongest correlation with brine release volumes under gas dominated flow regimes. There does not appear to be any relationship between brine release and saturation under brine dominated flow regimes in the CRA-2019, and only a weak correlation exists in the RPPCR. For the gas dominated flows, the sensitivity of DBR volume to mobile brine saturation in the RPPCR is about one third the CRA-2019 sensitivity, with about the same correlation.

Taken together, these results indicate: (i) if brine saturation is low so that the flow is gas dominated, then DBR intrusions are more sensitive to panel saturation than they are to panel pressure; and (ii) if brine saturation increases enough to produce a brine dominated flow regime, then panel brine

[2] SciPy is a Python-based ecosystem of open-source software for mathematics, science, and engineering. https://www.scipy.org

[3] For the CRA-2019, just 13 simulations yielded a gas relative permeability of zero: the all brine straight line in Figure 15 (top) is a fit through 13 points.

Information Only

saturation becomes less important and DBR volumes are more sensitive to panel brine pressure. Fully saturated panels in the CRA-2019 are sensitive to both panel saturation and panel pressure.

Figure 17 shows the frequency of non-zero DBRs versus mobile brine saturation for the S2-DBR scenario at the L and M intrusion locations. In Section 4.3 it was noted that the frequency of non-zero DBRs at these locations is about the same in the CRA-2019 and the RPPCR, and that the mean release volume in the RPPCR is about one third the mean in the CRA-2019. Figure 17 indicates more DBRs are occurring at lower panel saturations in the RPPCR at the L and M locations. Figure 18 shows the DBR frequencies at the U and O intrusion locations. Compared to the CRA-2019, frequencies have increased for all saturations at the U intrusion location; however, the numbers are small. There are also a small number of DBRs at the O intrusion location in the RPPCR.

Information Only

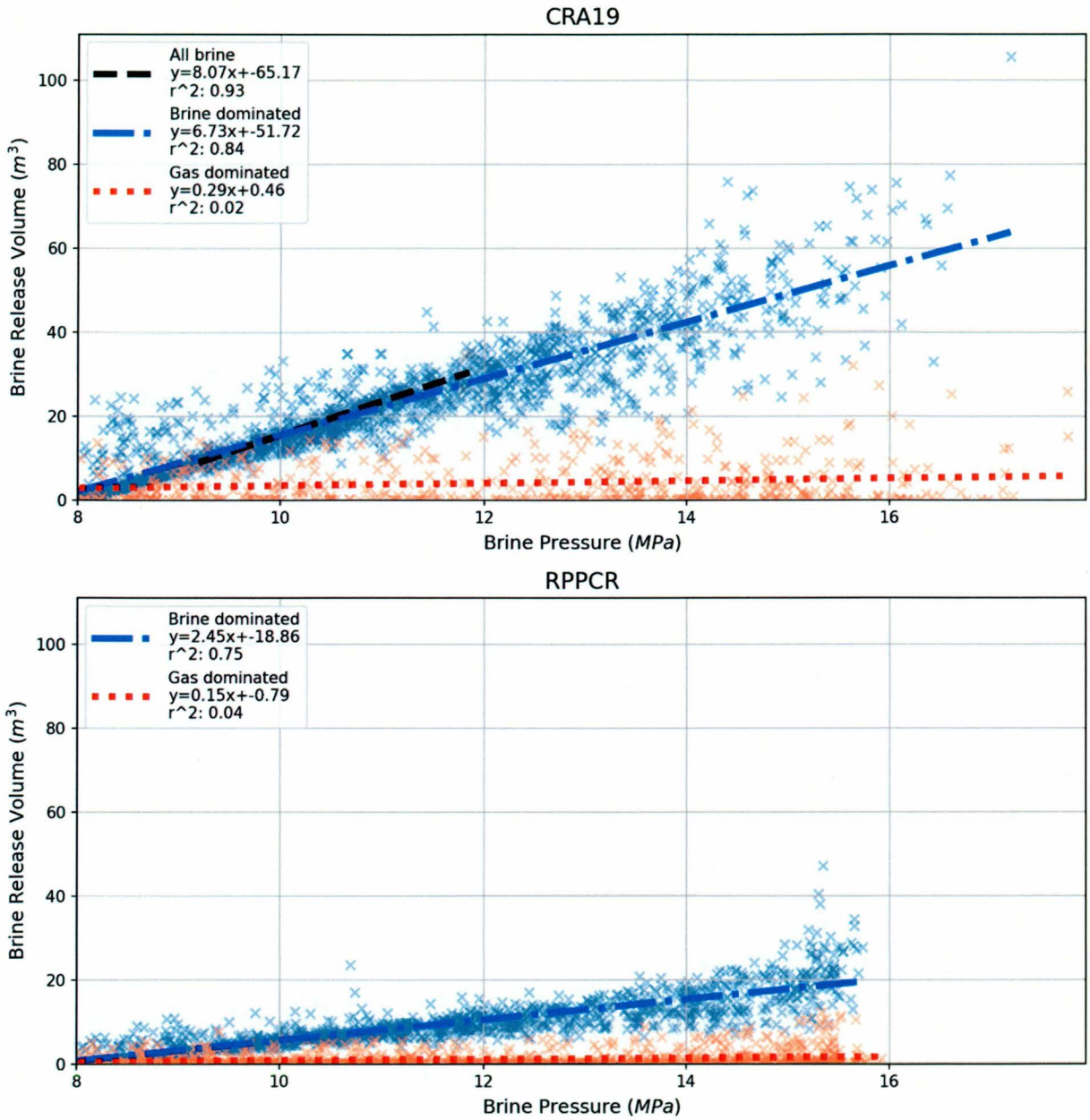


Figure 15: S2-DBR release volume versus brine pressure, all non-zero intrusions

Information Only

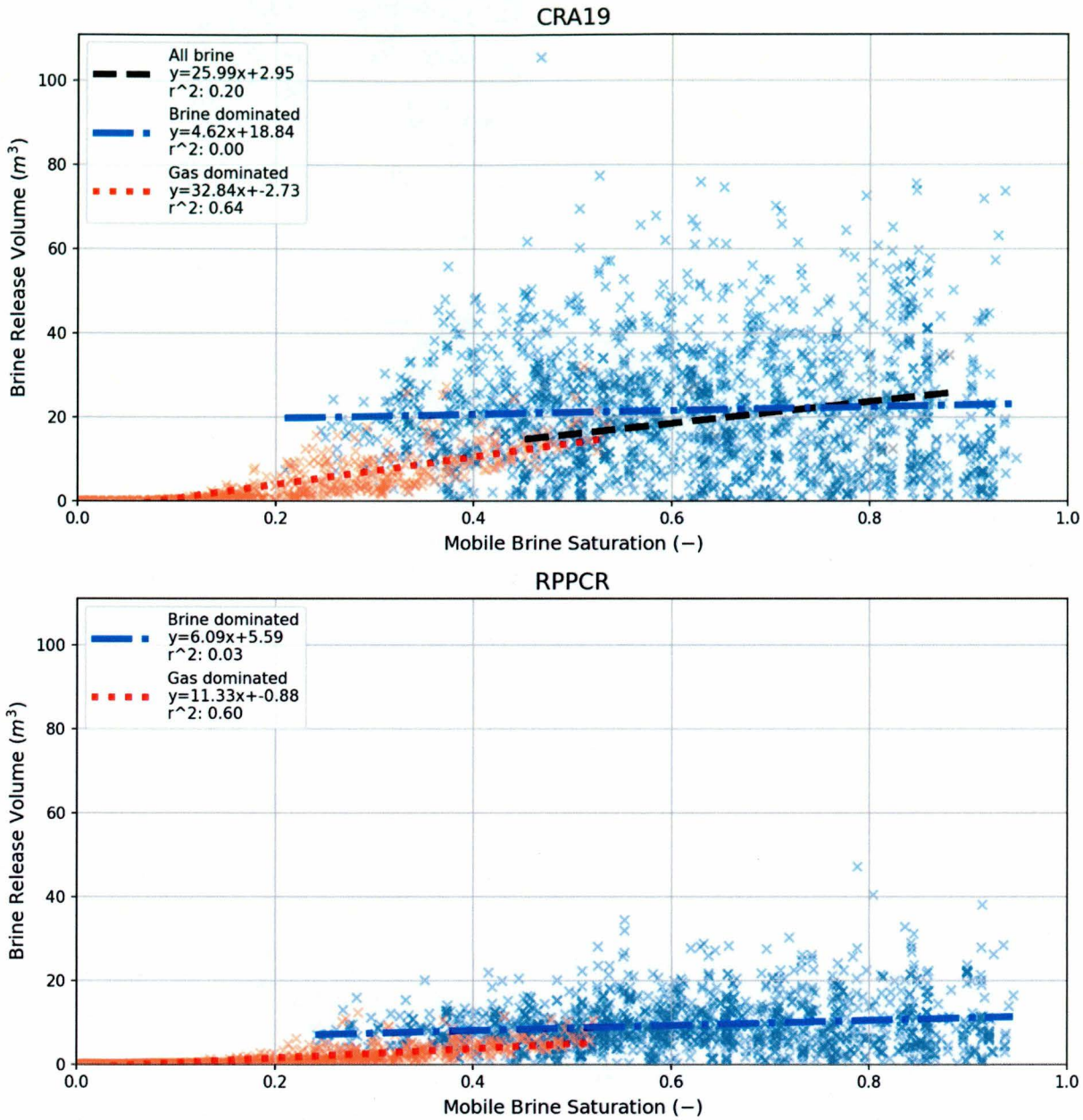


Figure 16: S2-DBR release volume versus brine saturation, all non-zero intrusions

Information Only

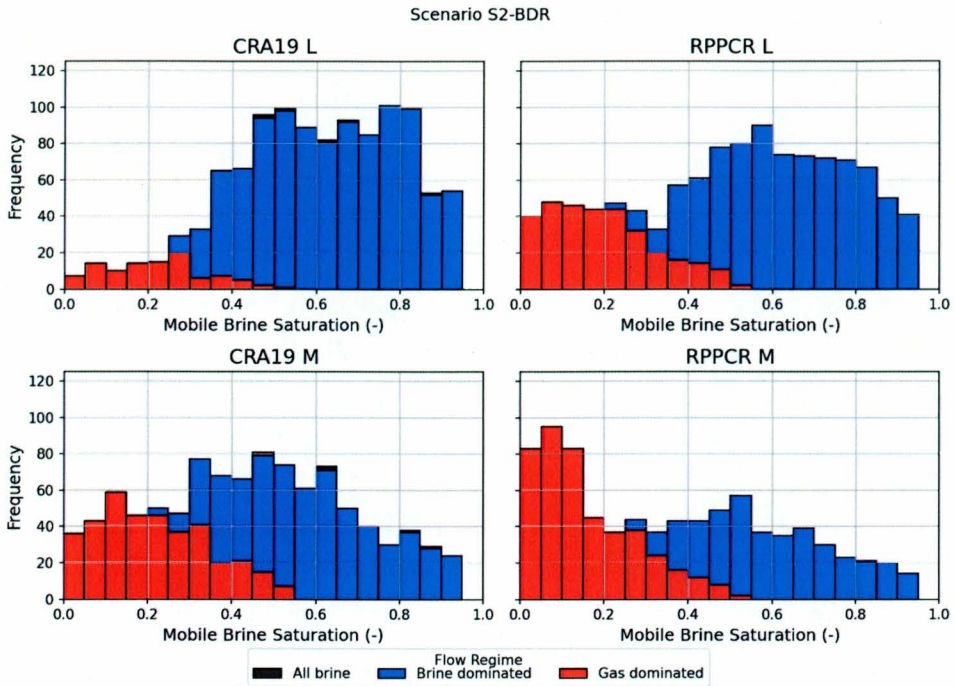


Figure 17: Brine saturation frequency, S2-DBR all Lower and Middle intrusions

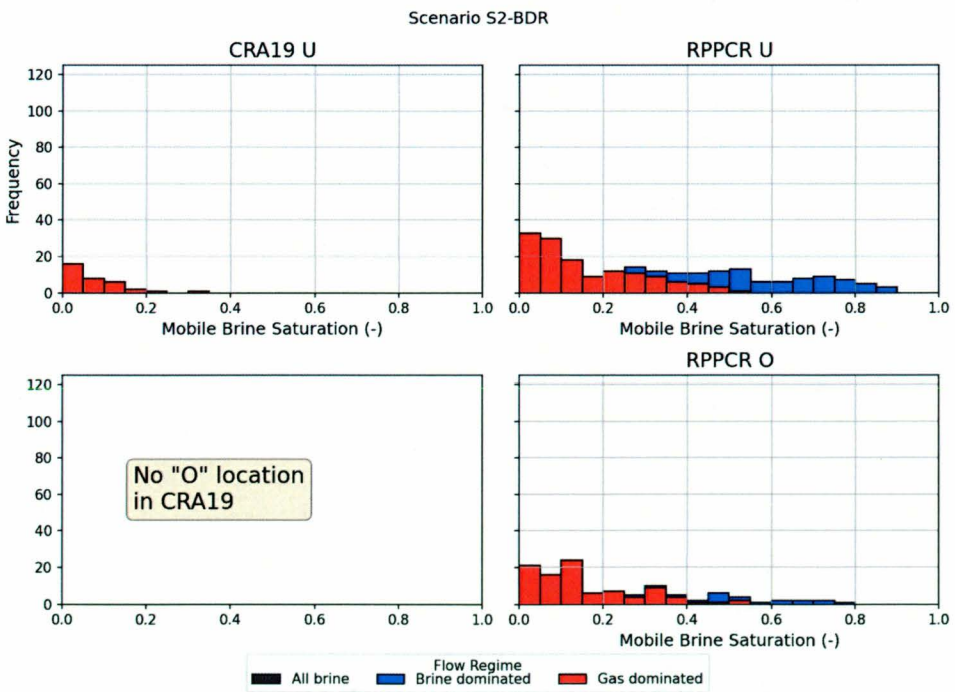


Figure 18: Brine saturation frequency, S2-DBR all Upper and Other intrusions

Information Only

5.3 Comparison to Other Analyses

Two PA analyses were carried out between the CRA-2019 and the RPPCR: the Additional Panels Performance Assessment (APPA) and the Replacement Panels Performance Assessment (RPPA). Due to the many changes between the CRA-2019 and the RPPCR, the APPA and RPPA analyses will be used here to further understand what model changes drive the largest changes in DBR volumes.

The APPA (Hansen, 2020) included the replacement and additional panels (Panels 11-19), the parameter updates associated with these new panels, and the updates to the DBR grid to account for the new panels. The DBR volume results were reported by King (2021).

The RPPA (Hansen, 2022) included an updated inventory closer to the inventory used in the RPPCR and the new methodology for calculating iron surface area for iron corrosion, in addition to the changes implemented in the APPA. The DBR volume results were reported by King (2022).

Table 9 shows brine release statistics and Figure 19 shows the brine volumes from non-zero DBRs for the CRA-2019, APPA, RPPA, and RPPCR analyses. While there are slight differences between the CRA-2019, APPA, and RPPA results, the major shift towards smaller release volumes is unique to the RPPCR analysis. From this it can be concluded that the changes implemented in the APPA and the RPPA are not the major drivers for changes seen in the RPPCR. Stated differently, neither the inclusion of the replacement and additional panels, nor the change to iron surface area, are drivers for the major changes in DBRs seen in the RPPCR DBRs.

Table 9 – DBR volume summary

Intrusion Location	Mean Brine Released (m^3)				Fraction of Simulations with Non-Zero Releases				Mean of Non-Zero Brine Releases (m^3)			
	CRA19	APPA	RPPA	RPPCR	CRA19	APPA	RPPA	RPPCR	CRA19	APPA	RPPA	RPPCR
S1-DBR	0.26	0.38	0.31	0.58	2.54%	4.12%	3.35%	9.58%	10.11	9.28	9.11	6.03
S2-DBR	8.29	5.82	5.6	2.18	47.22%	37.23%	35.95%	37.90%	17.55	15.64	15.57	5.76
S3-DBR	5.23	3.48	3.43	1.43	40.44%	30.72%	30.52%	33.22%	12.94	11.34	11.24	4.31
S4-DBR	0.07	0.15	0.11	0.78	1.04%	2.22%	1.85%	12.72%	7.14	6.60	6.08	6.11
S5-DBR	0.12	0.24	0.19	1.02	1.62%	3.48%	2.97%	14.88%	7.70	7.00	6.52	6.84
All Scenarios												
L	5.37	4.98	4.94	2.94	29.33%	29.73%	29.47%	38.68%	18.29	16.75	16.77	7.60
M	2.72	2.76	2.46	1.08	23.38%	24.58%	23.54%	24.85%	11.65	11.25	10.46	4.34
U	0.00	0.07	0.06	0.52	1.15%	4.31%	3.51%	12.83%	0.18	1.55	1.64	4.06
O	-	0.00	0.00	0.16	-	1.85%	1.40%	8.42%	-	0.07	0.02	1.86
L, M, and U	2.70	2.60	2.49	1.51	17.96%	19.54%	18.84%	25.45%	15.02	13.32	13.20	5.94
ALL	2.70	1.95	1.87	1.17	17.96%	15.12%	14.48%	21.20%	15.02	12.92	12.88	5.54

Information Only

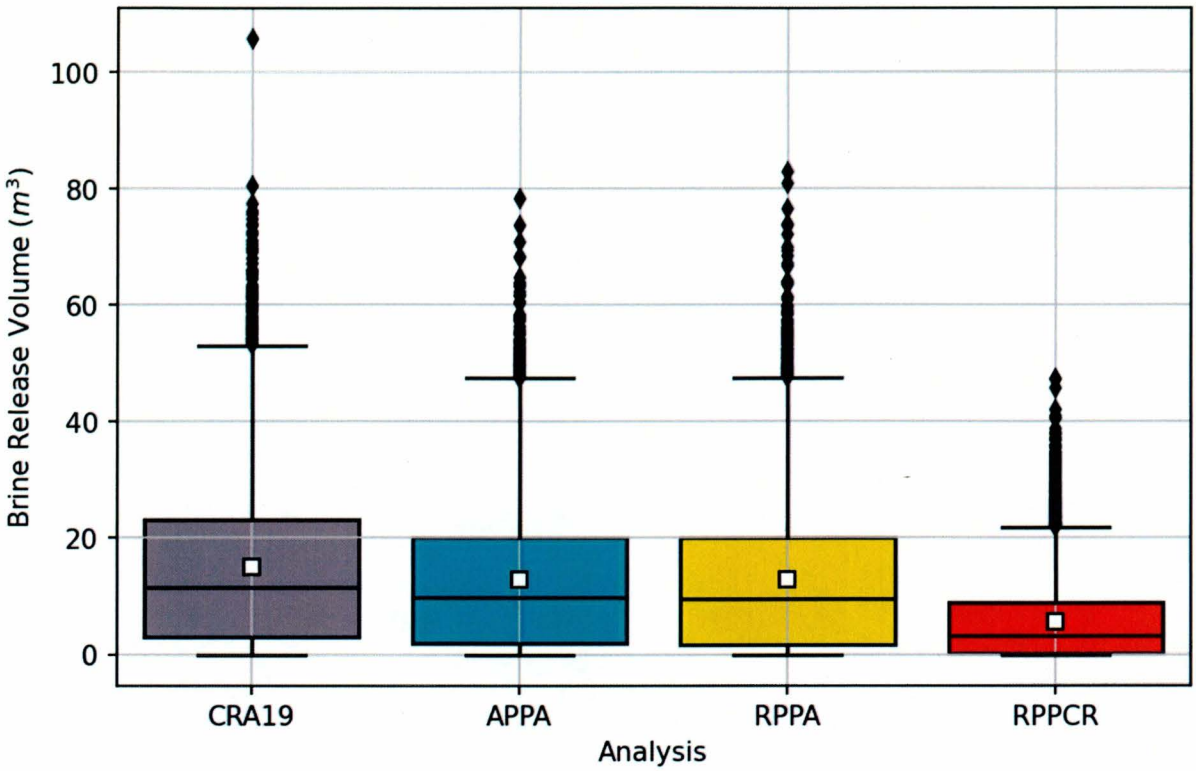


Figure 19: Brine release volumes for all non-zero DBRs.

Changes unique to the RPPCR that could drive the major changes to the brine release volumes are:

- the updated porosity surface to model creep closure of the salt,
- the updated borehole permeability,
- the updated actinide baseline solubilities and solubility uncertainty distributions, and
- the revised model for the oxidation states of actinides.

Given that the actinide baseline solubilities, solubility uncertainty distributions, and oxidation state models only impact the brine release volumes through the brine radiolysis model, which is a minor component of total gas generations with minimal impact to brine pressure or saturation, those changes can be ruled out as the cause of the major shift in brine release volume results. The updated borehole permeability affects brine pressure and saturation in scenarios with an intrusion, particularly in scenarios with an E2 intrusion (S4-BF and S5-BF). However, given the shift in DBRs in the undisturbed scenario where the borehole permeability is not used (see Figure 8), it is most likely that the update to the porosity surface is the primary driver for the shift in brine release volumes in the RPPCR, which is in alignment with the conclusions stated in King (2023).

Information Only

This page intentionally left blank.

Information Only

6.0 SUMMARY

The extended repository area included in the RPPCR representation of the WIPP introduced a need to model an additional panel intrusion location for the DBR calculation. With the short duration of DBR simulations, there is very little communication across panel closures; therefore, there is not a need to preserve an explicit representation of repository volume outside of the panel closures containing the intrusion locations. With this, the North Rest-of-Repository in the DBR grid is split into two regions: the Upper waste region, which contains the U borehole intrusion location; and the Other waste region, which contains the new O borehole intrusion location. A second key change incorporated into the RPPCR is an update to the porosity surface. Used to model the effects of creep closure in the waste area on fluid flow in and around the repository, the porosity surface affects both initial brine pressure and saturation in the DBR grid.

Compared to the CRA-2019, the number of non-zero DBRs increased significantly in the RPPCR; however, these were mostly small magnitude releases. The number of large magnitude releases decreased in the RPPCR. The increase in the number of non-zero DBRs came mostly from scenarios that did not involve a previous E1 intrusion.

The mean release volume in the RPPCR fell to about one third the mean release volume in the CRA-2019. The drop in release volume was most significant for the E1 intrusion scenarios; this, combined with the greater number of DBRs in the non-E1 scenarios mentioned above, meant there was less variation across intrusion scenarios in the RPPCR compared to the CRA-2019.

In both the RPPCR and the CRA-2019, the largest DBRs occurred at the L borehole intrusion location, situated in the down-dip Lower waste region. DBRs from the new O borehole location in the RPPCR made up only a small fraction of the DBRs from all intrusion locations.

The RPPCR Salado flow model (King, 2023) showed an increase in mean and median brine pressure and, for scenarios without a previous E1 intrusion, an increase in brine saturation. The increase in the number of non-zero DBRs in the RPPCR is attributed to these Salado flow conditions.

The RPPCR Salado flow model also indicated a reduction in the maximum brine pressure and, for scenarios involving a previous E1 intrusion, a reduction in brine saturation. The decrease in large magnitude DBRs, and the overall reduction in DBR volumes, is attributed to these Salado flow conditions.

The updated porosity surface in the RPPCR significantly reduces mean porosities in the waste area, so that the final pore volume is roughly half that realized in the CRA-2019 (King, 2023). For scenarios without a previous E1 intrusion, the reduced porosity creates higher saturations in the RPPCR; this, combined with increased inventory, increases gas generation and drives waste pressures up. For scenarios with a previous E1 intrusion, the smaller pore volume in the RPPCR means less brine can enter the waste following the intrusion; then, though initially high, saturation falls as the smaller volume of brine is consumed by chemical reactions. The reduced brine saturation at later times in the RPPCR E1 scenarios will tend to counteract gas generation due to the increased inventory, and thus counteract higher pressures.

Information Only

This page intentionally left blank.

Information Only

7.0 REFERENCES

Bethune, J. 2019. Analysis Package for Direct Brine Releases in the 2019 Compliance Recertification Application Performance Assessment (CRA-2019 PA). ERMS 571370. Carlsbad, NM: Sandia National Laboratories.

Brooks, R.H. and A.T. Corey. 1964. Hydraulic properties of porous media, Hydrology Paper no. 3. Fort Collins, CO: Civil Engineering Department, Colorado State University.

Brunell, S., C. Hansen, D. Kicker, S. Kim, S. King, and J. Long, 2021. Summary Report for the 2020 Additional Panels Performance Assessment (APPA). ERMS 574494. Carlsbad, NM: Sandia National Laboratories.

Chappelear, J.E., and A.S. Williamson. 1981. Representing Wells in Numerical Reservoir Simulation: Part 2—Implementation. Society of Petroleum Engineers Journal, vol. 21: 339–44.

Clayton, D.J., S. Dunagan, J.W. Garner, A.E. Ismail, T.B. Kirchner, G.R. Kirkes, M.B. Nemer. 2008. Summary Report of the 2009 Compliance Recertification Application Performance Assessment. ERMS 548862. Carlsbad, NM: Sandia National Laboratories.

Falta, R., M. Hu, E. M. Kwicklis, C. I. Steefel, S. C. Williams-Stroud, and J. A. Thies. 2021. Additional Panels Performance Assessment (APPA) Changed Conceptual Models Peer Review Report. Carlsbad, NM: U.S. Department of Energy, Carlsbad Field Office.

Hansen, C. 2020. Analysis Plan for the Additional Panels Performance Assessment. AP-185. Carlsbad, NM: Sandia National Laboratories. ERMS 573557.

Hansen, C. 2022. Analysis Plan for the Replacement Panels Performance Assessment. AP-193. Sandia National Laboratories. Carlsbad, NM. ERMS 576579.

Hansen, C., S. King, J. Bethune, and S. Brunell. 2023. Analysis Plan for the Performance Assessment for Replacement Panels Planned Change Request. AP-204. ERMS 579449. Carlsbad, NM: Sandia National Laboratories.

Helton, J.C., J.E. Bean, J.W. Berglund, F.J. Davis, K. Economy, J.W. Garner, J.D. Johnson, R.J., MacKinnon, J. Miller, D.G. O'Brien, J.L. Ramsey, J.D. Schreiber, A. Shinta, L.N. Smith, D.M. Stoelzel, C. Stockman, and P. Vaughn. 1998. Uncertainty and Sensitivity Analysis Results Obtained in the 1996 Performance Assessment for the Waste Isolation Pilot Plant. SAND98-0365. ERMS 252619.Albuquerque, NM: Sandia National Laboratories.

King, S. 2021. Analysis Package for Direct Brine Release in the Additional Panels Performance Assessment (APPA). ERMS 574498. Carlsbad, NM: Sandia National Laboratories.

King, S. 2022. Direct Brine Release Analysis Report for the Replacement Panels Performance Assessment (RPPA). ERMS 577306. Carlsbad, NM: Sandia National Laboratories.

King, S. 2023. Salado Flow Analysis Report for the Replacement Panels Planned Change Request (RPPCR). ERMS 579722. Carlsbad, NM: Sandia National Laboratories.

Kirkes, R. 2007. Evaluation of the Duration of Direct Brine Release in WIPP Performance Assessment (Revision 0). ERMS 545988. Carlsbad, NM: Sandia National Laboratories.

Information Only

Long, J. 2023. Computational Code Execution and File Management for the Replacement Panels Planned Change Request (RPPCR). Carlsbad, NM: Sandia National Laboratories. ERMS 579728.

MacKinnon, R.J., and G. Freeze. 1997a. Summary of EPA-Mandated Performance Assessment Verification Test (Replicate 1) and Comparison with the Compliance Certification Application Calculations, Revision 1. ERMS 422595. Carlsbad, NM: Sandia National Laboratories.

MacKinnon, R.J., and G. Freeze. 1997b. Summary of Uncertainty and Sensitivity Analysis Results for the EPA-Mandated Performance Assessment Verification Test, Rev. 1. ERMS 420669. Carlsbad, NM: Sandia National Laboratories.

MacKinnon, R.J., and G. Freeze. 1997c. Supplemental Summary of EPA-Mandated Performance Assessment Verification Test (All Replicates) and Comparison with the Compliance Certification Application Calculations, Revision 1. ERMS 414880. Sandia National Laboratories, Carlsbad, NM.

Mattax, C.C. and R.L. Dalton. 1990. Reservoir Simulation. Richardson, TX: Henry L. Doherty Memorial Fund of AIME, Society of Petroleum Engineers.

Shumaker, N. 2021. Relationship between DBR volume and placement of wellbore intrusion in upper panels. ERMS 576148. Carlsbad, NM: Sandia National Laboratories.

Stoelzel, D.M., and D.G. O'Brien. 1996. Analysis Package for the BRAGFLO Direct Release Calculations (Task 4) of the Performance Assessment Calculations Supporting the Compliance Certification Application (CCA), AP-029, Brine Release Calculations. ERMS 417870. Albuquerque, NM: Sandia National Laboratories.

US Department of Energy (DOE). 1996. Title 40 CFR Part 191 Compliance Certification Application for the Waste Isolation Pilot Plant (October). Carlsbad, NM: Carlsbad Area Office. DOE/CAO-1994-2184.

U.S. Environmental Protection Agency (EPA). 1998. 40 CFR 194, Criteria for the Certification and Recertification of the Waste Isolation Pilot Plant's Compliance with the Disposal Regulations: Certification Decision: Final Rule, Federal Register. Vol. 63, 27354-27406.

U.S. Environmental Protection Agency (EPA). 2022a. Overview of EPA Review of U.S. Department of Energy 2019 WIPP Compliance Recertification Application Performance Assessment. EPA-HQ-OAR-2019-0534. Washington, D.C.: U.S. Environmental Protection Agency, Office of Radiation, and Indoor Air.

Zeitler, T.R., J. Bethune, S. Brunell, B. Day, D. Kicker, J. Long, and R. Sarathi. 2019. Summary Report for the 2019 Compliance Recertification Application Performance Assessment (CRA-2019 PA). ERMS 571376. Carlsbad, NM: Sandia National Laboratories

Information Only

8.0 APPENDIX A: SENSITIVITY TO INPUT PARAMETERS

Brine pressure and saturation are the two most important drivers of DBR volumes, consequently the sampled parameters that control variability in brine pressure and saturation also control variability in DBR volumes. Since scenarios with a previous E1 intrusion drive non-zero DBRs, dominant parameters affecting waste panel pressure and saturation for the Salado Flow RPPCR S2-BF scenario are discussed in this Appendix. The dominant parameters were determined using a STEPWISE analysis (King, 2023).

For waste panel pressure in the RPPCR S2-BF scenario, the intact halite porosity parameter S_HALITE:POROSITY is dominant, followed by the long-term borehole permeability BH_SAND:PRMX_LOG, and the probability of plastic and rubber biodegradation parameter WAS_AREA:PROBDEG (King, 2023). For waste panel saturation in the RPPCR S2-BF scenario, the list of impactful parameters is longer; also, no single parameter dominates. The list includes: S_HALITE:POROSITY; the DRZ permeability parameter DRZ_1:PRMX_LOG; the waste residual brine saturation WAS_AREA:SAT_RBRN; Castile brine pressure CASTILER:PRESSURE; and factors controlling gas generation and brine consumption such as the iron corrosion rate parameter STEEL:CORRMCO2.

Scatter plots illustrating the sensitivity of DBR volumes to four of these parameters are shown in Figures 20-23. Increased intact halite porosity, which is associated with both increased waste panel pressure and saturation in the RPPCR S2-BF scenario (King, 2023), tends also to cause an increase in DBRs (Figure 20). Borehole permeability, which is inversely related to waste panel pressure (King, 2023), shows no obvious correlation to DBR volume (Figure 21). The correlation between higher values of permeability in the DRZ and DBRs is likewise weak (Figure 22). Lastly, at intrusion times near the time of the previous intrusion, higher pressure in the intersected Castile brine pocket drives higher repository pressure as brine from the Castile floods the repository, strongly affecting DBR volumes. The relationship between the Castile brine pressure and S2-DBR brine releases at time 550 years (200 years post-initial intrusion) is shown in Figure 23.

Information Only

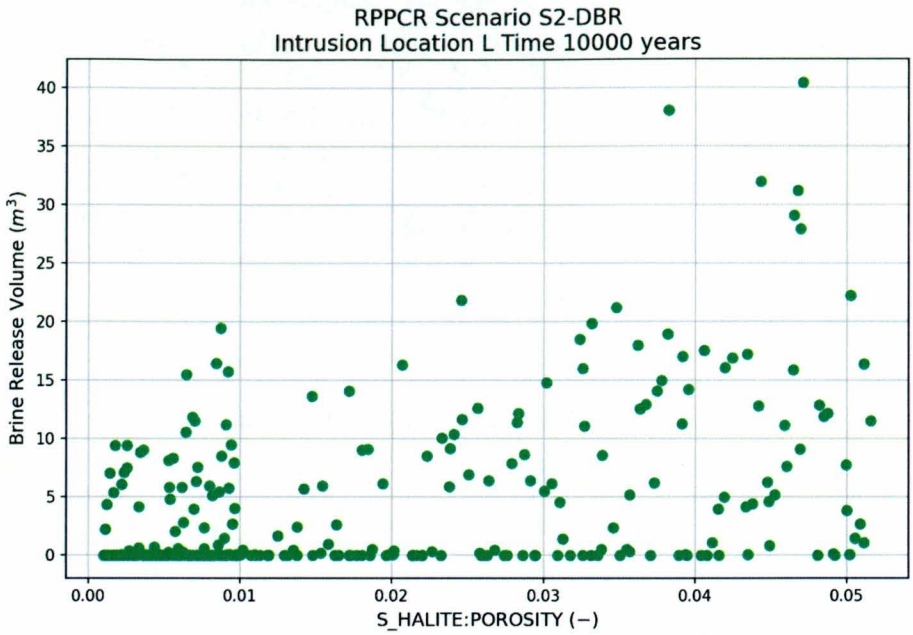


Figure 20: Halite porosity versus brine release volume for Location "L", Scenario S2-DBR, time 10,000 years

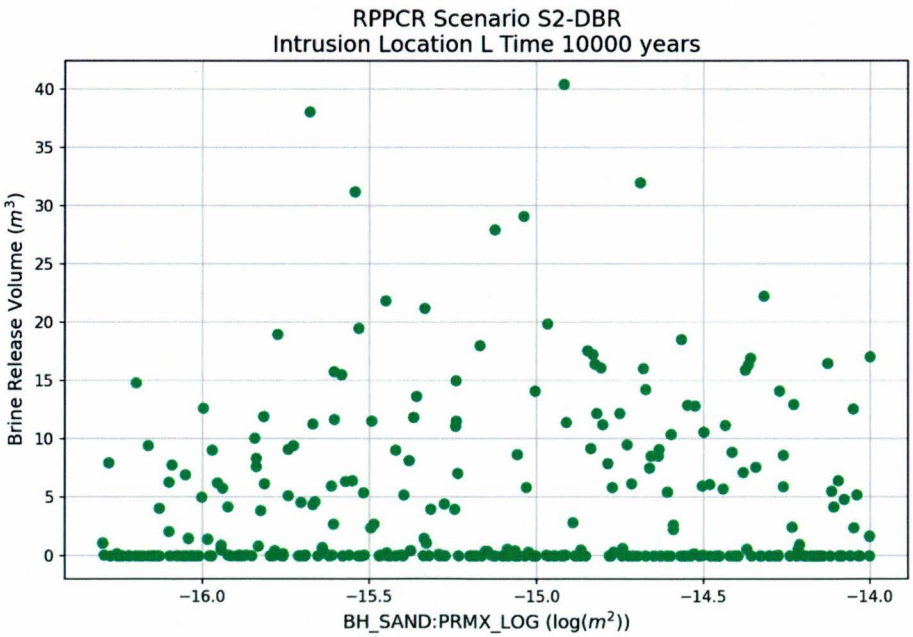


Figure 21: Borehole permeability versus brine release volume for Location "L", Scenario S2-DBR, time 10,000 years

Information Only

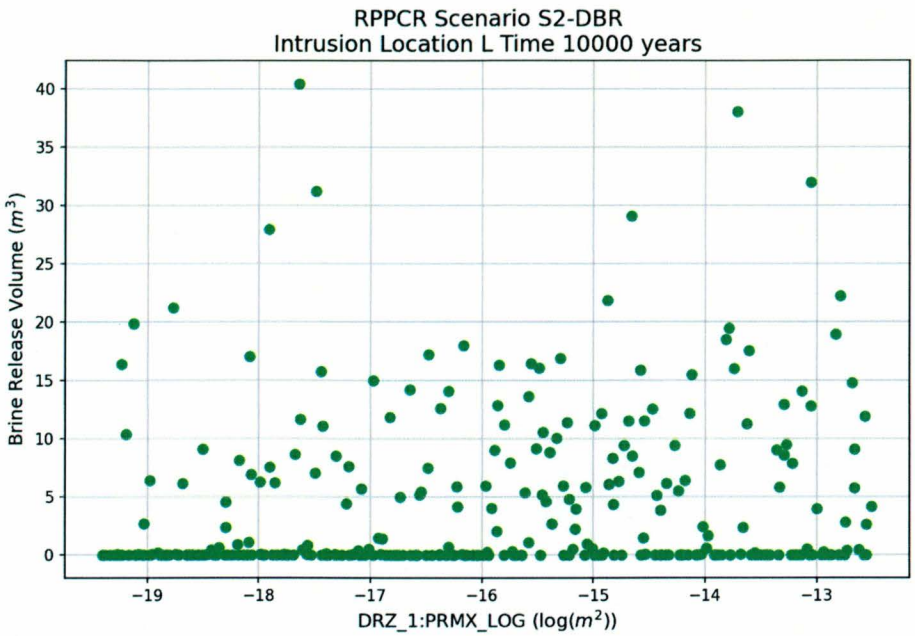


Figure 22: DRZ permeability versus brine release volume for Location "L", Scenario S2-DBR, time 10,000 years

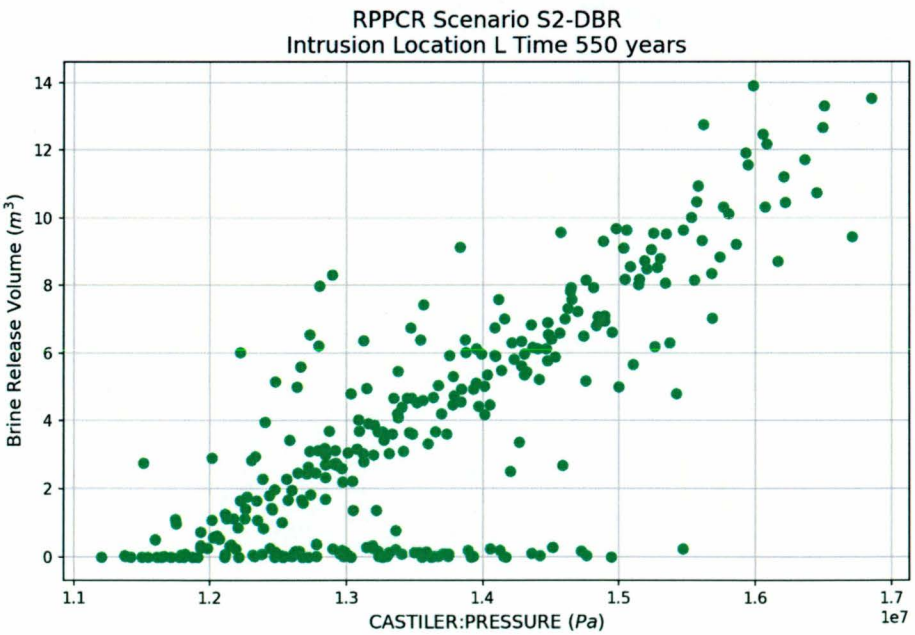


Figure 23: Castile brine pressure versus brine release volume for Location "L", Scenario S2-DBR, time 550 years

Information Only

This page intentionally left blank.

Information Only